Iceberg Production and Characteristics at the Termini of Tidewater Glaciers around the Prince of Wales Icefield, Ellesmere Island

Abigail Dalton

Thesis submitted to the
Faculty of Graduate and Postdoctoral Studies
in partial fulfillment of the requirements
for the M.Sc. Degree in Physical Geography

Department of Geography
Faculty of Arts
University of Ottawa

Supervisor:
Dr. Luke Copland

Thesis Committee:

Dr. Anders Knudby

Dr. Adrienne Tivy

Table of Contents

Abstract

Since the 1960s, warming air and sea surface temperatures have led to decreasing sea ice extent and longer periods of open water in the Canadian Arctic Archipelago (CAA). Recent and rapid changes have also been observed in the ice discharge patterns of glaciers in this region. For example, Trinity and Wykeham glaciers on the Prince of Wales Icefield (POW), SE Ellesmere Island, contributed ~62% of total ice discharge to the ocean from the Canadian Arctic Archipelago in 2016, compared to ~22% in 2000. Given these changes, an important question is whether there is a relationship between changing sea ice conditions (e.g., extent, freeze up dates, break up dates) and iceberg production from these glaciers.

This study used synthetic aperture radar (Radarsat-1, 2 and ALOS PALSAR) and optical (Landsat-7 and 8) imagery to identify iceberg plume events and sea ice break-up/freeze-up dates between 1997 and 2015 for 40 tidewater glaciers around the POW. Results show a clear relationship between the presence of sea ice and the production of icebergs from glaciers, with most events occurring during the open water season and fewer when sea ice was present. While there have not been clear increasing trends of icebergs produced from all glaciers in the POW, Trinity and Wykeham glaciers show that increases in detected iceberg plumes coincide with increases in previously measured glacier velocity and significant terminus retreat. Comparison to ocean temperature, surface air temperature from NCEP/NCAR reanalysis and tidal data showed no clear relationship with increased calving events, however further research into all factors is recommended. It is likely that there are several factors contributing to the spatial and temporal variability of iceberg production from the POW.

Acknowledgements

Support for this research has been provided by the University of Ottawa, the Canadian Ice Service (CIS), Natural Resources Canada (Program of Energy Research and Development), ArcticNet, the Northern Scientific Training Program, the Canadian Space Agency (Radarsat Constellation Mission Data Utilization and Application Plan), MEOPAR, Canada Foundation for Innovation, Ontario Research Fund, Polar Continental Shelf Program and Transport Canada. Support for travel to conferences and attendance of courses was generously provided by the ArcticNet Training Fund, GlacioEx and the High North Fellowship.

Firstly, I would like to thank the Canadian Ice Service for help with collection of data and for providing me with access to the Radarsat image archive. In particular, Dr. Adrienne Tivy for her help during my time at CIS and for her support as a thesis committee member. I would also like to thank thesis committee member Dr. Anders Knudby for his help and comments through this process. I would like to acknowledge the Canadian Coast Guard and scientific crew of the CCGS Amundsen for their assistance during fieldwork. I would also like to thank my fellow members of the Laboratory for Cryospheric Research and fellow cryosphere colleagues for their guidance throughout my project. I appreciated your company and encouragement in the field and your continual friendship and advice back in the lab.

I would like to thank my supervisor, Dr. Luke Copland, for his constant support, inspiration and guidance throughout this entire process. Luke introduced me to the world of glaciology and has provided me with countless opportunities that I never could have imagined to conduct fieldwork, present my research and discover my love for the Arctic. For all of this I am incredibly grateful.

Lastly, I would like to thank my friends and family for their unwavering support throughout this journey. I am very grateful to my parents Chris and Debbie Dalton for always encouraging me to work hard and to pursue my dreams. I want to thank my sisters Justine and Elise for paving the way and continuing to inspire me. Thank you!

List of Figures

List of Tables

Chapter 1: Introduction

Over the past 40 years, rapid warming has been observed in the Arctic, at a rate twice as fast as the global average (Cohen et al., 2014). This has occurred partly due to polar amplification, which in turn has been caused primarily by a reduction in sea ice cover (Screen & Simmonds, 2010; Serreze & Barry, 2011). Since the 1960s, Central Arctic sea ice extent has decreased by 8.6% decade^{-1} during the summer and thickness at the end of melt season has decreased by about 1.6 m between 1958 and 2007, when at the beginning of this period ice thicknesses ranged between 3.24 to 3.88 m (Stroeve et al., 2008; Stroeve et al., 2014). These changes have been observed in most of the Canadian Arctic as a result of warming air and sea surface temperatures, leading to longer periods of open water. Arctic warming has also had a significant impact on floating and land ice masses. For example, air temperatures have increased at a rate of 0.5°C decade^{-1} on northern Ellesmere Island since the late 1940s, contributing to the rapid loss of ice shelves there (White et al., 2015). The Ellesmere region of the Canadian Arctic Archipelago (CAA) has undergone an acceleration in ice loss through both calving and surface melt since 2003 and as a result has been the largest contributor to sea level rise outside of the Greenland and Antarctic Ice Sheets over this period (Harig and Simons, 2016).

Tidewater glaciers drain glaciers, ice caps and ice sheets, and terminate in the ocean where they discharge ice through the calving of icebergs (Vieli & Nick, 2011). Previous work has been conducted on the location of the main tidewater glaciers in Canada, their surface velocities, and the volumes of ice that they discharge to the ocean, but little research has been undertaken on the processes controlling iceberg production (Van Wychen et al., 2014; Van Wychen et al., 2016). Recent and rapid changes have been observed in the ice discharge patterns of glaciers in this region. For example, Trinity and Wykeham glaciers on the Prince of Wales Icefield on SE

Ellesmere Island contributed ~62% of total solid ice discharge to the ocean from the Canadian Arctic Archipelago in 2016, compared to ~22% in 2000 (Van Wychen et al., 2016).

In southern Canadian waters (e.g., east coast of Newfoundland), the Canadian Ice Service (CIS) produces charts to identify iceberg presence for navigational purposes. However, there is uncertainty surrounding the origin of these icebergs as CIS does not monitor their sources, which hampers long-term forecasting and the accuracy of iceberg drift models. A better understanding is therefore required of which tidewater glaciers are the sources of icebergs in Canadian waters, whether iceberg discharge rates are changing in response to variable sea-ice conditions, glacier dynamics or external forcing, and whether there have been changes in the magnitude and frequency of iceberg calving events over the past couple of decades.

1.2 Project Objectives

Using the study period 1997-2015, this project will address the following questions to determine which processes are driving iceberg production from SE Ellesmere Island:

1) Does the timing, frequency or magnitude of iceberg production from tidewater glaciers flowing from the Prince of Wales Icefield (POW) change seasonally or inter-annually?
2) Have sea ice conditions near the terminus of tidewater glaciers around the POW changed between 1997 and 2015, and is there a connection between changing sea ice conditions (e.g., freeze-up dates and break-up dates) and iceberg production from these glaciers?
3) Is there a relationship between measured glacier velocity changes (Van Wychen et al., 2014; Van Wychen et al., 2016) and iceberg production from tidewater glaciers in the POW?

4) Is there a relationship between climatic and/or tidal variations and changes in iceberg production from the POW?

The period 1997-2015 was chosen for the focus of this study as it coincides with the availability of Radarsat-1 and 2 SAR (synthetic aperture radar) satellite imagery and is accessible from the CIS archive through a joint project agreement. Radarsat-1 and 2 imagery comprises the majority of the 8400+ scenes used for this analysis. SAR imagery provides coverage for the Canadian Arctic during all times of year and in all weather conditions. ALOS-PALSAR and Sentinel 1A SAR imagery was also used to supplement the dataset. Open access Landsat-5, 7 and 8 optical satellite imagery from 1997-2015 was also used for higher resolution validation of SAR imagery results.

1.3 Area of Interest

The Prince of Wales Icefield is located on SE Ellesmere Island and contains approximately 73 tidewater glaciers (Sharp et al., 2014). The locations of the largest of these glaciers are indicated in Figure 1. Rapid recent increases in the surface velocity of Trinity and Wykeham Glaciers, the two largest outlet glaciers from POW, has resulted in a doubling of their ice flux to the ocean over the past decade (Van Wychen et al., 2016). Given their regional importance, the methodology for this project was developed based on identification of iceberg production, sea ice conditions and changes in terminus extent for these two ice masses. Trinity and Wykeham Glaciers are located in Talbot Fiord and terminate to the east towards Baffin Bay. To place the calving from these ice masses in perspective, and to understand regional controls on iceberg production, this study also quantifies iceberg production from all tidewater glaciers in the POW with a terminus width >1 km, of which there are 40 (Figure 1).

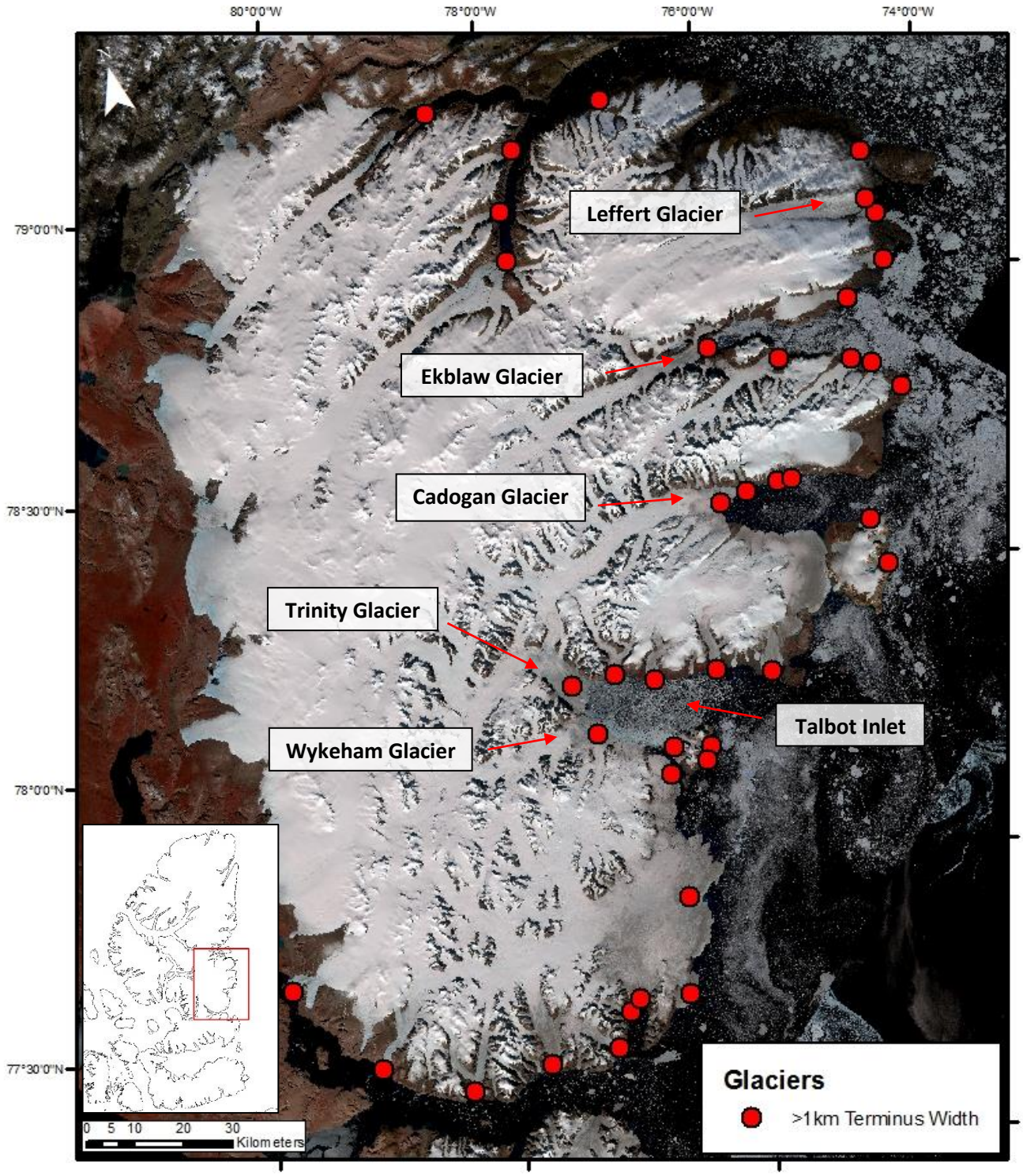

Figure 1.1: Map of the Prince of Wales Icefield on SE Ellesmere Island highlighting major glaciers as well as all tidewater glaciers with termini widths >1 km. Base image: USGS/NASA Landsat-8 Mosaic, July/August/September 2015.

Chapter 2: Background

2.1 Sea Ice

2.1.1 Seasonal Sea Ice Trends

Since the late 1960s summer sea ice extent has consistently decreased in most areas of the Arctic, including an acceleration in decrease over the past ~15 years (Stroeve et al., 2008; Stroeve et al., 2014; Serreze & Stroeve, 2015; Simmonds, 2015). This decrease correlates with warming of both sea surface temperature (SST) and surface air temperature (SAT) (Stroeve et al., 2008; Stroeve et al., 2014). Warmer temperatures have brought on earlier melt seasons and later freeze-up dates, creating a longer open water season (Stroeve et al., 2014). Longer periods of open water allow for increased heat absorption by the Arctic Ocean, increased sea surface temperatures and a delay in the onset of freezing, leading to decreased sea ice extent and thickness.

Sea ice extent has declined in all months since 1979, when the satellite record began. However, the most significant changes are being observed in September during the period of minimum annual sea ice extent (Stroeve et al., 2014; Simmonds, 2015). It is predicted that by approximately 2030 the Arctic will experience a nearly ice-free summer, except for ~1.0 million km^2 that will remain within the CAA compared to the 4 million km^2 that typically exists there at the end of the summer today (Wang et al., 2009; Serreze & Stroeve, 2015). As of 2014, 8 of the lowest September sea ice extents have occurred within the past 8 years (Serreze & Stroeve, 2015) (Figure 2.1). Decline in winter sea ice extent has been less than half that of summer (-3.1% and -8.6% per decade, respectively, over the past three decades), but it is still of great importance in determining the conditions and behaviour of sea ice the following summer (Stroeve et al., 2008; Stroeve et al., 2014). Winter sea ice decline has been associated with increases in downward IR radiation from

1979-2011 caused by an influx of heat from lower latitudes as part of large-scale changes in oceanic circulation (Park et al., 2015).

As overall sea ice extent decreases, sea ice is also becoming thinner (Serreze & Stroeve, 2015). Since 1980, sea ice thickness in the central Arctic (including the Canada Basin, Nansen Basin and North Pole) has decreased on average by approximately 1.6 m at the end of melt season from 1958 to 2007. At the beginning of this period, ice thicknesses in the Central Arctic ranged between 3.24 and 3.88 m at the end of melt season (Kwok & Rothrock, 2009). Kwok & Rothrock (2009) also found that peak (i.e., midwinter) sea ice thickness has decreased from 3.64 m in 1980 to 1.89 m in 2008 over all regions. Prior to the beginning of the satellite era (1979), sea ice thicknesses was primarily determined from in situ observations such as sonar from submarines. However, these methods lacked a large spatial range. Long term trends of changes in sea ice thickness over large areas have therefore been measured since 2001 through projects such as Operation IceBridge and ICESat using LIDAR altimetry and radar techniques. These methods involved calculating changes in elevation and snow depth on top of an ice surface to determine changes ice thickness (Lindsay & Schweiger, 2015).

As of 2015, the oldest remaining sea ice in the Arctic is located along the northern coast of Ellesmere Island and within the islands of the QEI (Howell et al., 2013; Serreze & Stroeve, 2015). This occurs because ocean currents and variations in atmospheric pressure promote ice motion in the Arctic Ocean towards this region with the Beaufort Gyre. In the summer months when many channels within the QEI are ice free, there is typically an inward flux of MYI (multi-year ice) from the Arctic Ocean (Howell et al., 2013).

2.1.2 Multiyear Sea Ice

First year ice (FYI) refers to sea ice that has not survived past one winter's growth, while multiyear ice (MYI) refers to sea ice that has survived at least one summer melting cycle (CIS, 2005; Maslanik et al., 2011). In the 1980s, the Arctic Ocean contained about 20% MYI of age five years and older, compared to 2014 when <5% of MYI was older than five years (Serreze, 2015). Since 1979, there has been a steepening trend of decreasing sea ice thicknesses and age over the Arctic Ocean that is consistent with increasing sea surface and surface air temperatures (Stroeve et al., 2014; Serreze & Stroeve, 2015).

The rate of SST warming has accelerated since 2000, contributing to earlier melt onset dates and later freeze-up dates for sea ice (Stroeve et al., 2014). As a result, MYI is becoming younger and therefore thinner, making it more susceptible to complete melt during the summer months when temperatures peak (Maslanik et al., 2011; Serreze & Stroeve, 2015). Between 1980 and 2011, MYI extent decreased by ~50% during September and ~33% during March (Maslanik et al., 2011). Maslanik et al (2011) used satellite and buoy data to detect the start of a significant decrease in the oldest MYI types in the Arctic Ocean in 2006. This decrease in MYI extent continued until 2011, when a small recovery occurred, although ice thickness trends have continued to decrease into 2014 with little MYI replenishment (Kwok & Rothrock, 2009; Maslanik et al., 2011; Serreze & Stroeve, 2015). The MYI recovery was weakest in the Canada Basin region (which borders the QEI), which has seen a decline in MYI coverage by 83% between 2002 and 2009 (Maslanik et al., 2011).

Changes in MYI extent in the Arctic can also be attributed to processes contributing to wind-driven sea ice transport into and out of the Arctic Ocean. Sea ice is primarily exported out of the Arctic Ocean through Fram Strait, to the east of Greenland, at a rate of about 700,000 km^2 per year

(Polyakov et al., 2012). Changes in sea level pressure (SLP) can both promote and weaken transport of MYI (Maslanik et al., 2011; Polyakov et al., 2012). The Arctic dipole anomaly sees a pattern in SLP that features high pressure over the Arctic and low pressure over Eurasia and seems to promote the transport of sea ice towards Fram Strait (Polyakov et al., 2012; Serreze & Stroeve, 2015). When in positive phase, the Arctic Oscillation (AO) creates an area of low pressure over the Arctic and is associated with a similar increase in transport of sea ice out of Fram Strait (Polyakov et al., 2012; Serreze & Stroeve, 2015). Wind driven export of sea ice out of the Arctic can have a larger impact on MYI extent when coupled with increased warming trends in the region (Polyakov et al., 2012).

2.1.3 Landfast Sea Ice

Landfast sea ice (also known as fast ice) refers to ice that forms and remains fixed to a coastline, ice wall or between grounded icebergs (CIS, 2005). In the Canadian Arctic, landfast sea ice forms in seasonal cycles in regions with varying water depths, such as between 8 and 30 m in the Beaufort Sea and 100 m on the shores of eastern Baffin Island (Mahoney et al., 2007). Landfast sea ice can form either "in-situ" when ocean water freezes in place or by freezing of existing sea ice floes to a shore (CIS, 2005). When existing floes are frozen to become landfast, the ice is then categorized by age. Landfast ice can extend anywhere from several metres to several hundred kilometres from the shore on which it forms.

In the CAA, landfast sea ice varies spatially throughout the year with some regions of sea ice remaining landfast for most of the year, while others are only landfast for about half of the sea ice season (Galley et al., 2012). High Arctic regions of the CAA typically become landfast by mid-

November, with most of the remaining southern regions becoming landfast in January (Galley et al., 2012). Breakup usually begins in mid-June where the southern regions are the earliest to breakup and the High Arctic regions last, if at all (Galley et al., 2012). Analysis of CIS weekly ice charts between 1983 and 2009 for the CAA have shown onset of landfast sea ice formation being delayed by 1-3 weeks per decade and advanced by ~0.5 weeks per decade in the Beaufort Sea and CAA-East sub regions, with generally negative trends in landfast sea ice duration over the eastern Arctic (Galley et al., 2012). A study conducted by Mahoney et al. (2007) attempted to relate changes in landfast sea ice conditions with oceanic and atmospheric circulation trends. Results show that the timing of landfast ice break up correlated more with atmospheric circulation (i.e., increasing air temperatures) than oceanic circulation and suggests a trend towards earlier melt onset.

2.1.4 Relationship between Sea Ice and Tidewater Glaciers

Fast ice that forms adjacent to ice shelves or marine-terminating glaciers can act as a barrier between the terrestrial ice mass and the open ocean, therefore promoting their long-term stability (Pope et al., 2012; Reeh et al., 2001). For example, significant losses of the Petersen Ice Shelf on NW Ellesmere Island occurred after the loss of adjacent multiyear landfast sea ice from Yelverton Bay, leaving open water at the ice shelf terminus for several days (Pope et al., 2012; White et al., 2015). Many studies have shown that first and multiyear landfast sea ice appear to have a similar buffering effect on the production of icebergs from tidewater glaciers in the CAA and Greenland, with the loss of sea ice resulting in increased mechanical ice discharge (Higgins, 1991; Reeh et al., 2001; Herdes et al., 2012; Carr et al., 2013).

Several studies have been conducted, primarily on Greenland glaciers, which have identified a relationship between the presence of sea ice and the stability of tidewater glaciers (Reeh et al., 2001; Herdes et al., 2012; Carr et al., 2013). Reeh et al. (2001) studied this relationship for the Nioghalvfjerdsfjorden Glacier located on NE Greenland, which is 80 km long with a 30 km wide terminus composed of 3 main ice tongues. Observational data, aerial photographs and satellite imagery was used to identify the retreat of 25 km of the floating glacier tongue between 1951 and 1963 and a major calving event in August 1997 where estimated ice volume loss was 7.4 km^3. This major calving event occurred after the breakup of the adjacent barrier fast ice referred to as Norske Øer Ice Barrier (NØIB). Prior to this event, the NØIB remained intact and no major iceberg calving or glacier breakup occurred. During these periods, the glacier was observed to advance through the sea ice, suggesting that the NØIB was holding the ice tongues in place and preventing calving. Reeh et al. (2001) concluded that the fast ice acted as a barrier to the glacier front and that surface melt caused by warmer climate conditions had thinned the glacier tongues, making them more susceptible to breakup.

A similar study was conducted by Carr et al. (2013) on NW Greenland, where the relationship between 10 glaciers and atmospheric, oceanic and glacier-specific controls was investigated. All glaciers in their study underwent retreat between 1993 and 2010. Results showed that between 1990 and 2010, mean SAT for the region increased by ~8ºC and summer/autumn sea ice concentrations declined, a trend which coincided with the start of glacial retreat and sea ice formation with glacial advance. Alison Glacier, which experienced the highest rate of retreat between 1993 and 2010 of all the glaciers studied, retreated consistently following increases in air temperatures and decreases in sea ice concentration at its terminus.

An ice mélange is a mixture of sea ice and densely packed calved icebergs, often found at the front of high latitude tidewater glaciers (Amundson et al., 2010). Similar to landfast sea ice, an ice mélange can act as a barrier that stabilizes the terminus front of a glacier and inhibit calving from occurring (Joughin et al., 2008; Howat et al., 2010; Amundson et al., 2010; Moon et al., 2015). As air and ocean temperatures increase towards late spring and sea ice begins to break up, the ice mélange is also then able to disintegrate. Once calving begins, the mélange continues to break up as open water allows for more calving and waves promote further disintegration (Howat et al., 2010; Amundson et al., 2010). Little work has been conducted in the CAA surrounding this topic, apart from Herdes et al. (2012), who investigated the relationship between iceberg plume events (caused by glacier calving) and ice mélange conditions for Fitzroy and Belcher glaciers on NE Devon Island. Timing, frequency and size of iceberg plumes were identified through analysis of Radarsat-1 ScanSAR Wide imagery and were compared to sea ice break-up and freeze-up dates determined from CIS weekly ice charts. Consistent with the findings of Reeh et al. (2001) and Carr et al. (2013), Herdes et al (2012) found that most iceberg calving events occurred during the open water season, soon after fast ice had broken up at the terminus and before it had re-frozen. A pattern was also identified which saw larger calving events occurring with higher frequency and magnitude during the open water season than when fast ice was present. Results showed that small/medium plumes occur nearly simultaneously with fast ice loss and large iceberg plumes typically occur within several days after this. Herdes et al. (2012) concluded that a direct relationship exists between the presence of sea ice and production of icebergs from Belcher and Fitzroy glaciers.

2.2 Glacier Dynamics

2.2.1 Glacier Velocity

Glacier fronts undergo seasonal and multi-year cycles of advance and retreat (Howat et al., 2010). Tidewater glaciers typically advance in the winter and early spring when temperatures are low and sea ice is present at the terminus of the glacier. Lower temperatures allow for the glacier terminus to thicken and sea ice acts as a barrier to stabilize the calving front (Howat et al., 2010; Amundson et al., 2010). In the late spring and summer, as temperatures increase and sea ice breaks out, calving rates also increase which can lead to a retreat in glacier front position (Howat et al., 2010).

Changes in glacial motion can be seen on seasonal and inter-annual scales. Seasonally, for most glaciers, velocity increases in the spring and summer when surface melt and runoff increases. As water percolates to the glacier bed, it creates an area of high pressure, leading to increased motion of the glacier (Moon et al., 2015). Fast moving glaciers tend to have ponding of surface meltwater that percolates through crevasses while meltwater on slower moving glaciers tend to flow in streams along the sides and off the terminus (Williamson et al., 2008). As surface melt occurs, if water runoff is able to permeate the surface of the glacier through crevasses to the underlying bed, it can cause increased motion (Andersen et al., 2010; Vieli & Nick, 2011). Later in the melt season as a subglacial drainage system develops, it becomes more efficient. The same meltwater inputs then result in a lower subglacial water pressure and therefore glaciers typically experience a slowdown at the end of the summer (Moon et al., 2015).

Inter-annually, increases in glacier velocity have been attributed to increased surface melting that causes basal lubrication and therefore an increase in basal sliding (Howat et al., 2010). Studies in the CAA and NW Greenland have shown that changes in glacier velocity have occurred on both

tidewater glaciers and land-terminating glaciers since the 1990s, with the greatest increases being observed for tidewater glaciers (Joughin et al., 2008; Van Wychen et al., 2014). Glaciers that terminate on land can freeze to their beds leading to slower velocity compared to tidewater glaciers that terminate in water (Moon & Joughin, 2008; Van Wychen et al., 2012; Van Wychen et al., 2014). Higher glacier velocities can cause shearing, which produces crevasses (deep fractures in the glacier surface) (Vieli & Nick, 2011).

In the QEI, most tidewater glaciers have shown variable velocities over the past ~15 years, with periods of surging, pulsing and quiescence, but few long-term trends (Van Wychen et al, 2016). Only two glaciers in the QEI, Trinity and Wykeham glaciers on the Prince of Wales Icefield, have shown a consistent acceleration between 1999 and 2015 independent of a surge, with their iceberg discharge increasing from ~22% of the QEI total in 1999 compared to ~62% today. These changes in ice motion were measured using speckle tracking of pairs of RADAR images (Van Wychen et al., 2016). However, glacier mass losses in the QEI come from both iceberg calving and surface melting/runoff. Millan et al. (2017) found that from 1991-2015 mass loss from the QEI was on average 6.3 ± 1.1 Gt yr^{-1} where 52% was found to be from ice discharge (e.g., iceberg production) and the rest from surface mass balance (e.g., surface melt). However from 2005-2014, mass loss from ice discharge was on average 3.5 ± 0.2 Gt yr^{-1}, about 10%, compared to surface mass balance accounting for 90% or 29.6 ± 3.0 Gt yr^{-1}. Mass loss through iceberg calving therefore only represents a small portion of the total mass loss from the QEI today and surface melting and runoff also need to be considered when determining glacier mass balance in this region.

The POW has experienced increases in warming since 2005 and the calving flux combined with terminus retreat of the main outlet glaciers are responsible for -1.92 ± 0.21 Gt yr^{-1} of ice discharge (Sharp et al., 2014; Van Wychen et al., 2016). This compares to an average total mass loss (i.e.,

including surface melt) of 38 ± 2 Gt yr^{-1} with an acceleration of 8 ± 2 Gt yr^{-1} for the Ellesmere region over the period 2008-2015. Comparatively, between 2003 and 2015, Greenland experienced a mass loss over the entire sheet at an average rate of 244 ± 6 Gt yr^{-1}, with an acceleration rate of 28 ± 9 Gt yr^{-1} (Harig and Simons, 2016).

2.2.2 Oceanic Forcing

Unlike land terminating glaciers, tidewater glaciers are susceptible to both atmospheric and oceanic variability (Moon & Joughin, 2008; Howat et al., 2010; O'Leary & Christoffersen, 2013). As a result, increased SAT and SST can lead to melting of a tidewater glacier from both above and below (Moon & Joughin, 2008; Howat et al., 2010). While sea ice covers the ocean surface during the winter and early spring seasons, there is little to no exchange of heat between the air and ocean or ocean and glacier front (Walter et al., 2012). Maximum glacier terminus position occurs when a fiord is frozen with sea ice/icebergs, upwelling is minor and the glacier velocity is low (Motyka et al., 2003). Howat et al. (2010) conducted research on six tidewater glaciers in western Greenland and found that May SST warming over the last decade correlated to submarine melting of the glacier termini. They also found that a single season of anomalous ocean warming could trigger long-term instability of a glacier by reducing frontal advance and prolonging the open water season by preventing sea ice formation.

One of three of Greenland's largest outlet glaciers, Jakobshavn Isbrae (located on western Greenland), began a significant speed up and retreat in 1998 after being stable since 1950 (Joughin et al., 2008). Prior to 1997, ocean water temperature in this area had increased significantly at all depths (Motyka et al., 2011). After 1997, submarine melting was found to have increased by ~57

m yr^{-1} from the average summer melt rate of 228 ± 49 m yr^{-1} in 1984 and 1985, when thinning of the floating tongue was minimal. This increase in submarine melting occurred after a 1.1ºC increase in seawater temperature that occurred prior to this time, which continued to destabilize the floating glacier tongue and result in increased calving (Motyka et al., 2011; O'Leary & Christofferson, 2013). From 1997 to 2002, Jakobshavn Isbrae thinned at a rate of ~1.5 m yr^{-1}, mostly at the front of the glacier where velocity increased by ~70% in the first 20 km (Joughin et al., 2008).

Pinning or grounding of a glacier, when it is slowed by an obstacle such as the side of a fiord or bedrock below, can act to stabilize calving (Benn et al, 2007b). These pinning points can be lost when a glacier thins, reducing resistance and speeding up the flow (Joughin et al., 2008). Rapid acceleration of glacier velocity can then cause crevasses to form (Vieli & Nick, 2011), resulting in further calving, break-up of the glacier tongue and further weakening of the glacier front. As ocean temperatures surrounding western Greenland have increased, winter sea ice concentration fell from 100% in 1989-1996 to 50-60% in 2003. This created a longer open water season and allowed for warmer ocean waters to continue thinning the Jakobshavn Isbrae front and lead to the collapse of nearly its entire floating ice tongue (Joughin et al., 2008).

2.3 Iceberg Production

All iceberg calving results from crevasses caused by longitudinal strain or a decrease in ice thickness (Benn et al., 2007a; Benn et al., 2007b; Amundson et al., 2010). As ocean and air temperatures warm and the mélange weakens, the first icebergs of the melt season can begin to calve (Motyka et al., 2003; Amundson et al., 2010). The buttressing effect of the ice mélange

causes the first iceberg to break away bottom-out (Amundson et al., 2010). Once this iceberg has calved away, open water is left at the terminus of the glacier, decreasing the stabilizing impact of the ice mélange and allowing for subsequent icebergs to begin calving (Amundson et al., 2010). As the icebergs continue to calve, waves can act to further weaken the mélange causing break-up and reduction of back stress on the glacier front (Amundson et al., 2010; Howat et al., 2010).

Thinning of a glacier terminus through both surface and submarine melting means that iceberg calving can occur in several ways. Calving can result from undercutting of the terminus through basal melting along the bed of a grounded glacier or under a floating portion of the glacier (Amundson et al., 2010). Calving can also result from deep crevassing on the surface or underside of the glacier (Amundson et al, 2010). Several studies have highlighted the importance of an ice mélange or sea ice barrier to the stability of a glacier terminus and that a lack of back stress can lead to an increase in calving and therefore retreat of the glacier front (Reeh et al., 2001; Amundson et al., 2010; Howat et al., 2010; Herdes et al., 2012; Pope et al., 2012).

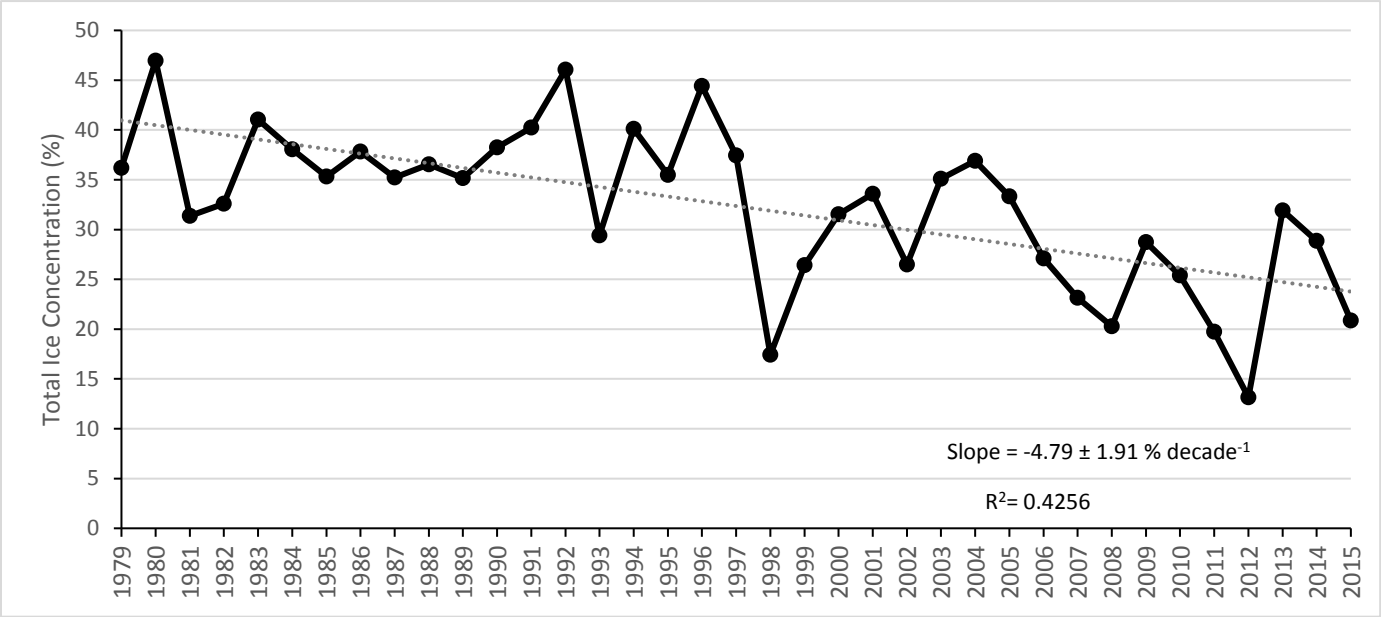

Figure 2.1: Canadian Arctic historical sea ice concentration for the end of September (same week 09/24), 1979-2015. Source: Canadian Ice Service (ECCC), 2017.

Chapter 3: Methodology

The primary objective of this project was to use satellite imagery and observational data to determine whether a relationship exists between climate, sea ice conditions and iceberg production from tidewater glaciers around POW between 1997 and 2015. Iceberg discharge patterns were quantified through manual analysis of iceberg production events and iceberg plumes identified in SAR and optical satellite images (Radarsat-1 and 2, ALOS-PALSAR, and Landsat-7 and 8), using a methodology based on that of Herdes et al. (2012). This analysis was completed for the 40 tidewater glaciers in the POW whose termini are >1 km in width (Figure 2.1). Connections between iceberg production and varying sea-ice conditions were evaluated by comparing the freeze-up/break-up dates of sea ice adjacent to glacier termini and the timing and characteristics of iceberg calving events.

Where possible, glaciers in the study area were identified using their official name as provided by the Geographical Names Board of Canada. However, where an official name was not available, they were identified using names provided by Van Wychen et al. (2014). Glaciers without an official name and not previously identified by Van Wychen et al. (2014) were named according to their location and proximity to other known glaciers.

3.1 Satellite Imagery

A total of 8426 scenes were collected between 1997 and 2015 for the POW (Table 3.1). Synthetic Aperture Radar (SAR) imagery was primarily used in this project for identifying iceberg plume events, with higher resolution optical imagery used when available. Scenes collected by the

following sensors were used for analysis in order to provide maximum spatial and temporal coverage for the area of interest (Table 3.1).

3.1.1 Radarsat-1 and 2

Synthetic aperture radar (SAR) imagery was primarily used in this project for identifying iceberg plume events. SAR imagery is a type of active microwave remote sensing that is sensitive to changes in surface roughness and melt through differing backscatter. Rough surfaces such as freshly calved glacier ice appear bright in SAR imagery due to high amounts of scattering, making it useful for the detection of iceberg plumes as they are able to be distinguished against the darker signature of open water or sea ice. SAR satellites, unlike optical, are able to acquire images during the day and night and can penetrate through cloud cover. Radarsat-1 and 2 are Canadian satellites launched in 1995 and 2007, respectively, and overlapped in their coverage between 2007 and 2013. Both satellites use the C-band frequency and collect imagery in multiple modes. Radarsat images were collected in ScanSAR Wide mode, which provides scenes with 100 m resolution and 500 km swath width. These images have been georectified using satellite orbital parameters to facilitate comparisons between them.

For the POW region, Radarsat-1 and Radarsat-2 SAR images in the CIS archive were available approximately every 1-3 days between June and October and every 1-2 weeks between November and May, providing year-round coverage. Herdes et al. (2012) used Radarsat-1 imagery to identify iceberg plume events from Belcher and Fitzroy glaciers on Devon Island. Their methods of identification and classification were used as a reference to create a methodology to classify and record iceberg plume events from the remaining tidewater glaciers of the POW for this project.

Radarsat-1 images were obtained from the CIS archive, the Alaska Satellite Facility (ASF) and National Earth Observation Data Framework Catalogue (NEODF) for the period 1997 to 2008 (approximately 3400 Radarsat-1 images for the area of interest). A joint project agreement with the CIS allowed access to approximately 4500 Radarsat-2 images over all areas of interest for 2009-2015.

3.1.2 ALOS-PALSAR

Additional SAR scenes from ALOS-PALSAR were collected to supplement the Radarsat archive and fill in periods of low temporal coverage. Images were collected in ScanSAR mode, which has a 100 m range resolution and a 250-350 km swath width. ALOS-PALSAR images are available through the ASF website and a total of 220 scenes were collected for the years 2007-2009. ALOS-PALSAR was a Japanese satellite that was active between 2006 and 2011 and collected imagery in the L-band frequency.

3.1.3 Landsat-7 and 8

Landsat satellites collect optical data, which is unable to penetrate cloud cover and requires daylight to see the surface. As a result, useable Landsat acquisitions are sporadic and typically occur between June and September each year. Landsat imagery is available in a panchromatic band with 15 m spatial resolution for Landsat-7 and Landsat-8, and was used to supplement the lower resolution SAR scenes. Landsat-7 and 8 scenes were acquired from the United States Geological Survey (USGS) through the online database EarthExplorer (http://earthexplorer.usgs.gov/) for

glaciers in the QEI between 1997 and 2015. Landsat-7 was used from 1999-2013 and Landsat-8 was used from 2013-2015.

3.2 Sensor Comparison

3.2.1 Detectability of Icebergs

When using multiple image sources, it is important to understand which features are, and are not, detectable in each one. When a calving event occurs from a glacier, smaller pieces of glacier ice typically break off with the main piece of calved ice. When these pieces break off and fall into the water, this produces what is known as a plume. Fresh iceberg plumes appear bright in SAR scenes because these surfaces are rough, particularly if the calving event is composed of small icebergs rather than one large iceberg or ice island. Surfaces that are wet or smooth, such as older sea ice or open water, appear dark in the SAR scenes, making the plumes distinguishable from the surrounding background (Herdes et al., 2012). Based on this, detected iceberg plume events are used to infer the production of icebergs from glaciers in the POW, even though the calving of singular icebergs is not clearly visible in SAR imagery.

To evaluate this methodology, a systematic comparison was made to quantify the sizes and characteristics of icebergs that can be detected with each sensor by comparing optical vs. SAR imagery used in this study and field observations collected on or around the same date. This helped to determine which types of imagery were suitable for iceberg plume analysis, and enabled an assessment of the limits and potential biases provided by the use of single types of satellite images.

No direct comparisons were possible for Prince of Wales Icefield due to lack of field data, so this analysis was undertaken based on observations and satellite imagery collected in July 2015 around

Yelverton Bay on northern Ellesmere Island. On July 13th, 2015, approximately 400 oblique photos and high resolution video were taken from a helicopter during fieldwork in this region; the location of these images was recorded and compared to Landsat-8 imagery and Radarsat-2 imagery acquired on July 19, 2015. These images were manually analysed and compared to the near simultaneous photos and video to identify and confirm the presence of icebergs in each scene. Once identified, each iceberg was then categorized based on the CIS MANICE iceberg length classification system: small (15-60 m), medium (61-120 m), large (121-200 m) and very large (>200 m). Through this assessment 2602 icebergs were identified and classified.

In the Landsat-8 imagery, 79% of iceberg detections were small or medium and size with the remaining 21% being large or very large. Higher resolution 15m panchromatic Landsat-8 imagery is well suited for detecting small, medium, large and very large icebergs in both open water and frozen in sea ice (Figure 3.1a). Iceberg freeboard refers to the portion of iceberg that is above sea level. Depending on the thickness of the iceberg, freeboard can vary greatly. As a result, some icebergs are nearly flush with the surrounding sea ice when frozen. Icebergs with and without freeboard were detectable in the Landsat-8 imagery. In the Radarsat ScanSAR imagery, none of the small or medium icebergs were identified, which is hardly surprising given that those icebergs are smaller than, or similar in size to, the 100 m ScanSAR image resolution (Figure 3.1b). For large and very large icebergs, a total of 69 icebergs (~42% large and 58% very large) were detected. Using Landsat imagery 299 large and 244 very large icebergs were detected, in addition to small and medium, meaning Radarsat was unable to detect 474 icebergs of this size. Detection of icebergs with little to no freeboard was generally unsuccessful using Radarsat-2 imagery.

This comparison demonstrated that Radarsat imagery is useful for covering large areas with high temporal coverage but in ScanSAR Wide mode it can only detect large and very large icebergs

(Figure 3.1a and b). It also highlighted the value of using optical imagery such as Landsat-8 for validation of iceberg detection in SAR imagery.

3.2.2 Detectability of Iceberg Plumes

Often when an iceberg calving event occurs an ice plume is produced from the terminus of the glacier, which is usually identifiable in SAR imagery due to its sensitivity to the backscatter produced by various surface types. This study uses the production of iceberg plumes to infer the production of icebergs from glaciers, so it is useful to gain an understanding of which sizes of plumes can be detected using remote sensing. This can be undertaken by comparing SAR image acquisitions to time-lapse photography of the terminus of Trinity Glacier available after August 2016.

Figures 3.2 and 3.3 show iceberg plumes being produced from Trinity Glacier on August 18 and 21, 2016. Figure 3.2e shows a near simultaneously acquired Sentinel 1A Extra-Wide SAR scene of 100m resolution from August 21, 2016, in which the plume produced in Figure 3.2 was not clearly detectable. Radarsat-2 and ALOS-PALSAR imagery was not available for this date, however it can provide similar useful information given that it uses the same resolution as the ScanSAR wide scenes that were predominantly used in this study.

Figure 3.3e shows a near simultaneously acquired Sentinel 1A SAR scene from August 18, 2016, where the plume produced in Figure 3.3 is clearly visible on the far side of the terminus as a bright spot. This comparison shows that some icebergs plumes are easily detectable in SAR imagery, while others are not and can be missed when conducting a plume analysis.

Since Landsat-8 imagery was not available with the same temporal and spatial coverage as Radarsat-2, it was determined that a combination of lower resolution Radarsat scenes and higher resolution Landsat scenes would be used to identify iceberg plume events. This would provide the most comprehensive coverage of the POW possible, while still taking into account the strengths and weaknesses of each sensor type.

The number of plumes identified in this study should be considered minimum estimates of the total produced. As previously discussed, small and medium sized icebergs (and plumes) are unable to be detected in lower resolution ScanSAR Wide imagery and Landsat-8 does not acquire imagery over the POW with the same frequency that would allow for it to be the sole sensor used for this study. Though Radarsat-1 and 2 have a high repeat rate over the Canadian Arctic, gaps remain in image acquisitions which can result in plume events being incorrectly identified if the plume occurred on a previous day or missed entirely.

3.3 Classification

For this project, iceberg calving events were classified through the identification of iceberg plumes and, in the case of Trinity and Wykeham Glaciers, through the measurement of glacier terminus changes. This maximized the ability to detect iceberg production events, as detailed below.

Based on the methodology of Herdes et al (2012), iceberg plume events were categorized into four size classifications: 1, 2, 3 and 4. Size 1 represents an iceberg plume which is approximately <1 km^2, size 2 represents a plume which is approximately 1-10 km^2, size 3 represents a plume that is approximately 10-20 km^2 and size 4 represents a plume that is approximately >20-30 km^2 (Figure 3.4). No events were detected with a plume size >30 km^2.

SAR and optical scenes were systematically analyzed manually for each year from 1997-2015, and all plume events were recorded. This analysis was completed for all 40 tidewater glaciers selected in the area of interest around POW. The approximate area of each plume was measured in ArcGIS in order to classify it as size 1, 2, 3 or 4 based on the system outlined above, and a note was made of which corresponding image it was detected in.

3.4 Terminus Changes

In addition to the identification of short-term plume events, the annual position of the terminus of Trinity and Wykeham glaciers was recorded for 1997-2015. Terminus outlines were drawn for each year on a date within a one to two week period at the end of summer (approximately September) using predominantly higher resolution Landsat 7 and 8 imagery, and Radarsat-1 ScanSAR imagery for earlier in the time series when there was no Landsat imagery available. At the end of summer, snow cover is at a minimum and there is little to no sea ice in fiords or at the glacier terminus, making it easily distinguishable in the imagery. Outlining the termini on approximately the same day each year accounts for the annual cycle of terminus advance and retreat experienced by many tidewater glaciers (Howat et al., 2010; Amundson et al., 2010).

The multi-year record of changes in terminus position was used to provide information concerning the influence of long-term climate changes on Trinity and Wykeham glaciers. This information was also required to enable an evaluation of how much iceberg production at the glacier terminus was the result of terminus retreat vs. steady-state ice flow. These outlines were added to previous observations of terminus change that were made periodically from 1959 to 1992 by W. Van Wychen using aerial photos and satellite imagery.

3.5 Sea Ice Freeze-up and Break-Up Patterns

The annual dates of sea ice freeze-up and break-up were determined to understand whether a relationship exists between the production of icebergs and the presence of sea ice. By determining these dates for 1997 to 2015, and for all glaciers in the study area, it helped to provide information as to whether the timing of these events has changed over the past 18 years.

Weekly ice charts were typically used in combination with the SAR and optical imagery to determine the freeze-up and break-up dates, although in a few cases when no SAR imagery was available the conditions reported in the charts were relied upon solely for identifying the timing. The online CIS archive of historical weekly ice charts for the Eastern Arctic (https://www.ec.gc.ca/glaces-ice/default.asp?lang=En&n=0A70E5EB-1) were used to identify the break-up date each summer as the period when the sea ice was no longer classified as 'landfast ice'. Conversely, sea ice freeze-up was identified as the period when sea ice was first classified as 'landfast ice' in the weekly charts. These changes in stage of development were based on the CIS MANICE classification system (identified as Form of Ice Code 8) (CIS, 2005). The classification of 'landfast' in CIS charts was chosen for this analysis (e.g., as opposed to a classification of 10/10 ice coverage), as landfast defines the time when ice is no longer able to move in a fiord. During plume analysis, approximate sea ice freeze-up and break-up dates were identified manually and used as validation for the sea ice charts which have lower resolution in smaller fiords. Manual analysis classified the sea ice break-up date as when sea ice had broken away from the terminus of the glacier and the freeze-up date as when there was no longer any movement of sea ice detected in the fiord.

To illustrate the conditions present at the terminus of Trinity Glacier when no landfast ice is present in CIS charts, Figure 3.5a shows a period when sea ice was completely broken out of the fiord

(September 30, 2016). Conversely, Figure 3.5b shows the terminus of Trinity Glacier when landfast sea ice is present at the terminus in the weekly ice charts (March 30, 2017).

The same dates of sea ice break-up and freeze-up were assigned to glaciers located in the same fiord or general region of the POW icefield (e.g., all glaciers located in Talbot Inlet).

3.6 Climate Data

National Centers for Environmental Prediction–National Center for Atmospheric Research (NCEP-NCAR) climate reanalysis data was used to extract seasonal mean surface air temperature for the CAA and more specifically the POW (https://www.esrl.noaa.gov/psd/data/gridded/data.ncep.reanalysis.html). This data was used to focus on the climatic conditions of the region during the open water season, when most of the iceberg plume events occur. Plots of mean seasonal surface air temperature anomaly data from June to September were created for each year from 1997 to 2015 to identify whether there are interannual spatial variations in surface temperature over the area of study. Mean seasonal data (June to September) from 1997 to 2015 for the POW was also plotted to identify any long-term trends in surface air temperature and help assess whether relationships exist between mean surface air temperature and iceberg plume events. Reanalysis data was used due to the lack of available observational data for this region. The nearest Environment Canada weather station is located in Grise Fiord (76°25′03″N 082°53′38″W), about 200 km south of Trinity and Wykeham glaciers. However, data collected at this station has large gaps in coverage and did not cover the full time period of the study.

3.7 Oceanic Data

There are few in situ measurements of ocean water temperatures in this region, particularly near glaciers. Data from the Copernicus Marine Environment Monitoring Service (CMEMS) TOPAZ4 ocean temperature model was therefore used to identify mean oceanic temperature at 50, 100 and 200 m depths for Baffin Bay and the CAA from 1991-2015. TOPAZ4 is a coupled ocean and sea ice data assimilation system that can be used to simulate the movement of water in the Arctic and forecast conditions such as ice thickness, salinity and water temperature (Sakov et al., 2012). Results were used to determine whether ocean temperatures vary with depth in the study region and whether a relationship exists between variations in ocean temperature and the production of icebergs from the POW. Processed data was obtained from A. Cook (University of Durham, UK) through personal communication (August, 2017).

3.8 Tidal Data

There are no tidal monitoring stations in the vicinity of POW, so a global tidal model data was used to predict historical tidal heights for this region. Data from the online WWW Tide/Current Predictor (http://tbone.biol.sc.edu/tide/tideshow.cgi) was used, which has been calibrated against past tidal measurements made in 1962 at Pim Island, Nunavut, located directly off the NE coast of the POW, about 1km from the coast and directly north of Leffert Glacier (78.0667° N, 74.0167° W). Tidal height data was analysed for 2011-2015 against timing of plume events from Trinity and Wykeham glaciers to determine whether a relationship exists between spring/neap tidal events and the production of icebergs. This five year time period was used to analyze the tidal events for Trinity and Wykeham glaciers because of the availability of data during that time. These five years

had the most satellite imagery available during the 18 year time period (Table 3.1) for detecting plume events and therefore offered the most data available for comparison with tide models.

Table 3.1: Comparison of type and number of satellite images analyzed for each year in this study.

	Radarsat-1	Radarsat-2	ALOS-PALSAR	Landsat-7	Landsat-8	Total
1997	194	-	-	-	-	194
1998	628	-	-	-	-	628
1999	383	-	-	12	-	395
2000	544	-	-	14	-	558
2001	421	-	-	13	-	434
2002	237	-	-	11	-	248
2003	231	-	-	3	-	234
2004	187	-	-	20	-	207
2005	159	-	-	22	-	181
2006	230	-	-	13	-	243
2007	131	-	55	33	-	219
2008	-	110	92	19	-	221
2009	-	205	73	27	-	305
2010	-	464	-	31	-	495
2011	-	712	-	23	-	735
2012	-	805	-	21	-	826
2013	-	920	-	8	19	947
2014	-	637	-	31	48	716
2015	-	580	-	-	60	640
Total	3345	4433	220	301	127	8426

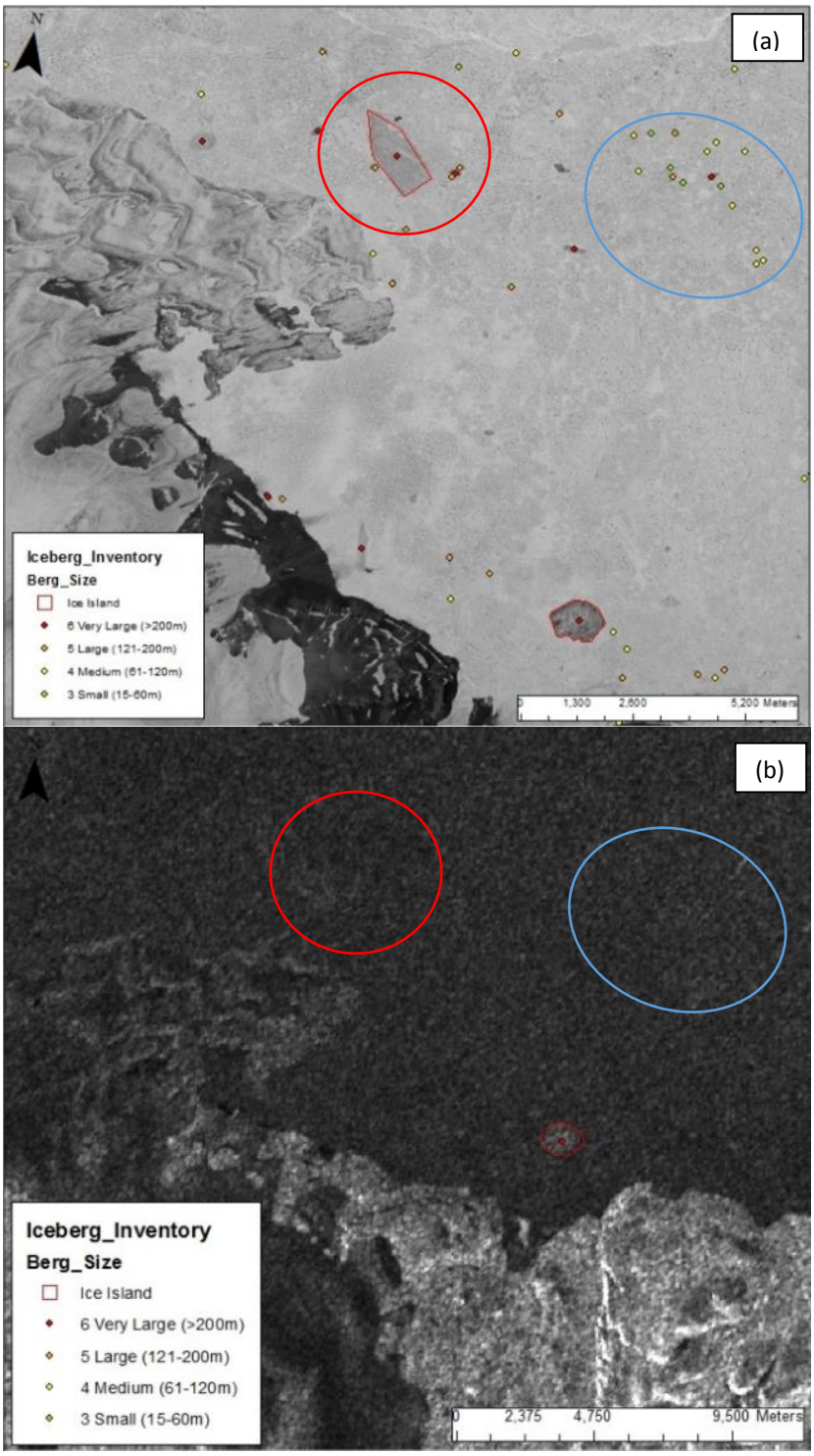

Figure 3.1: (a) Landsat-8 imagery acquired July 19 2015 showing small, medium, large and very large icebergs and two ice islands are visible in the optical imagery (b) Radarsat-2 image acquired July 19 2015 of the same region showing that the small and medium icebergs as well as one of the ice islands are not visible. RADARSAT-2 Data and Products © MacDONALD, DETTWILER AND ASSOCIATES LTD (2015) – All Rights Reserved. RADARSAT is an official mark of the Canadian Space Agency. USGS/NASA Landsat.

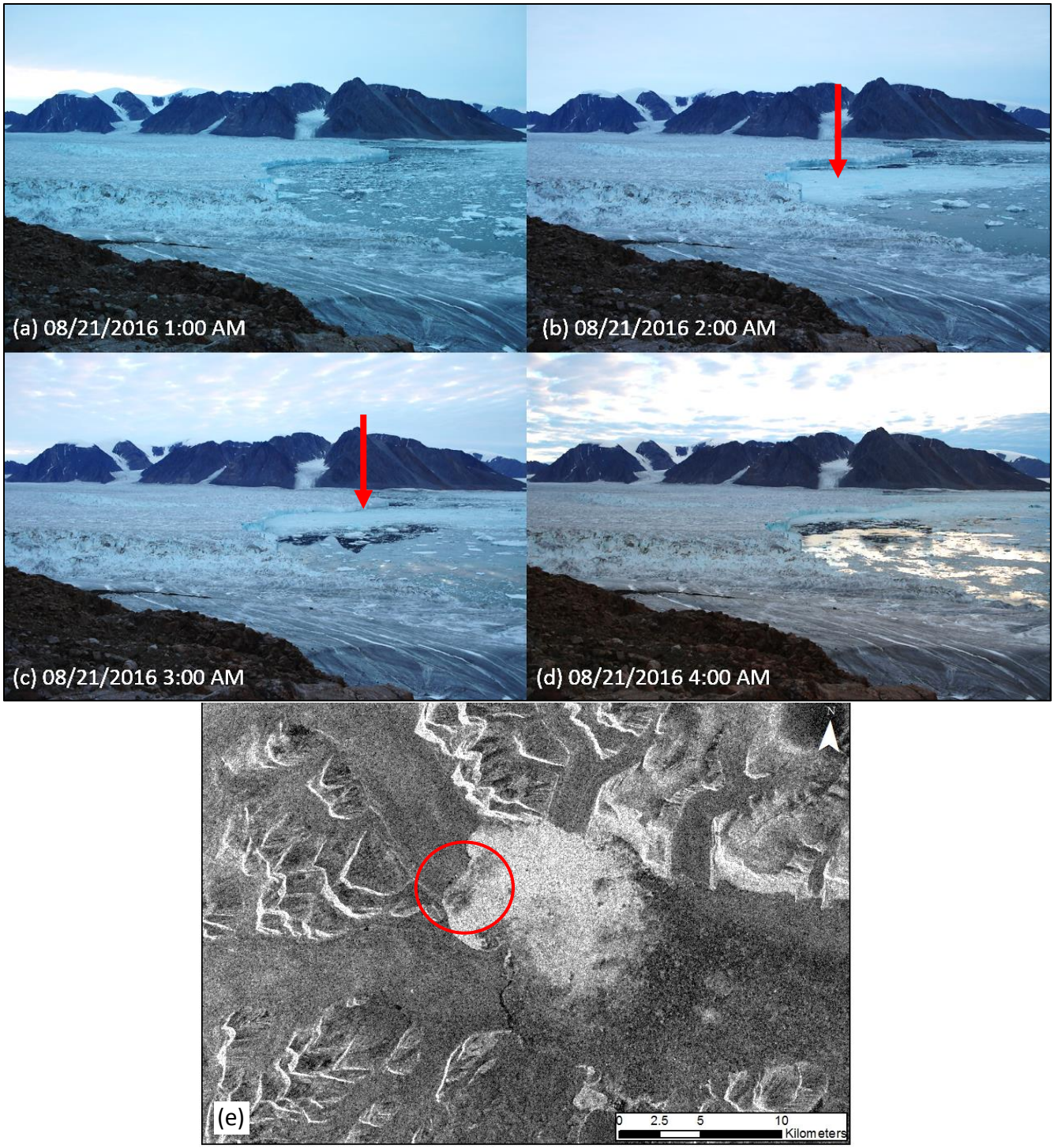

Figure 3.2: Iceberg calving event from time-lapse camera monitoring Trinity Glacier on August 21, 2016 from 1:00AM to 4:00AM. (a) pre-calving event; (b) calving event and appearance of iceberg plume; (c and d) dispersal of iceberg plume into Talbot Inlet; (e) Sentinel 1A SAR scene (acquired August 21, 2016 21:22:25) showing no detectable freshly calved plume from the terminus of Trinity Glacier (See Figure 3.2). Copernicus Sentinel Data, 2017.

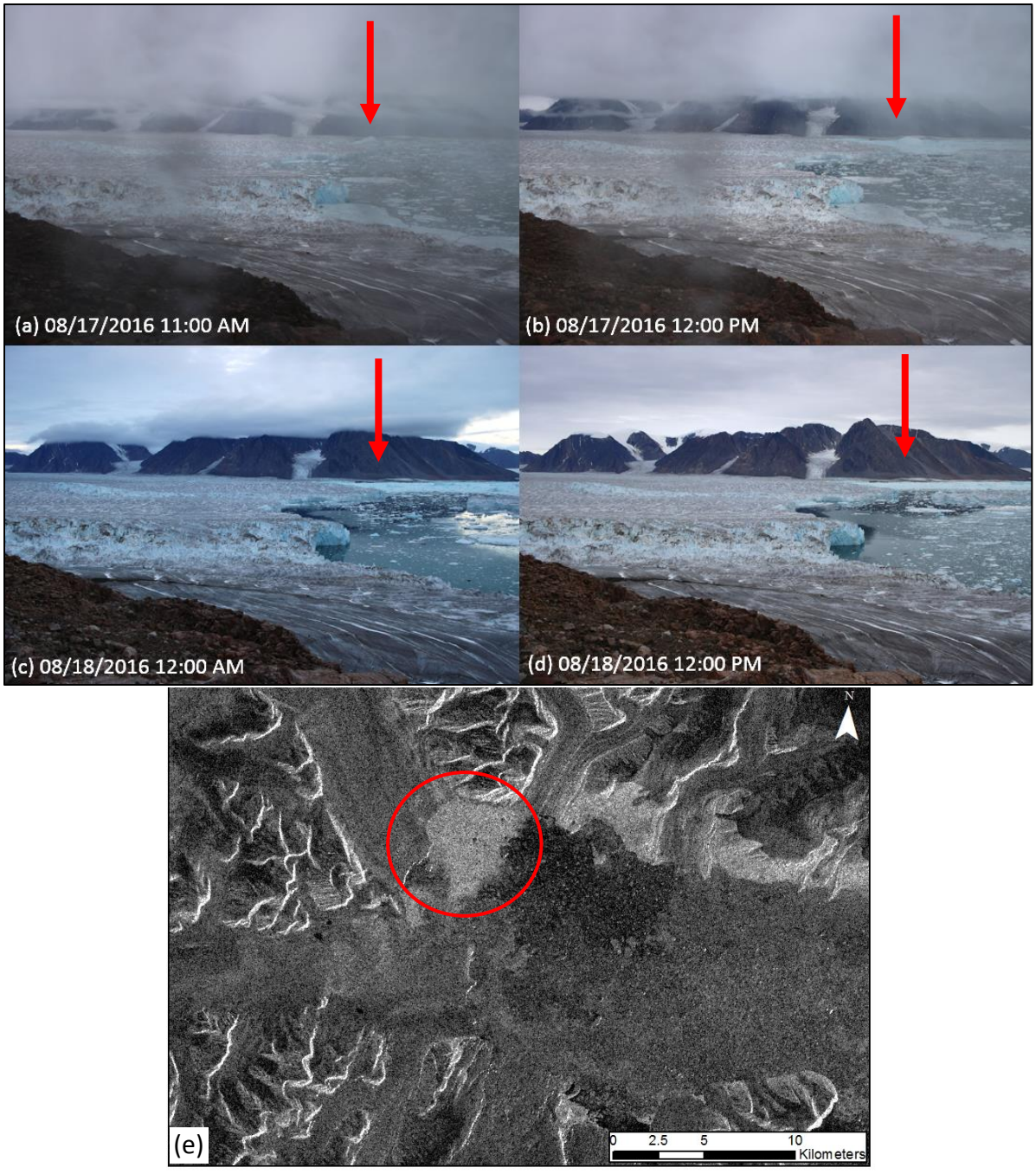

Figure 3.3: Iceberg calving event from time-lapse camera monitoring Trinity Glacier on August 18, 2016 from 11:00AM to 12:00PM. (a) pre-calving event; (b) calving event and appearance of iceberg plume; (c and d) dispersal of iceberg plume into Talbot Inlet; (d) Sentinel 1A SAR scene (acquired August 18, 2016 at 12:50:06) showing a clearly detectable plume on the north side of the terminus of Trinity Glacier (see Figure 3.4). Copernicus Sentinel Data, 2017.

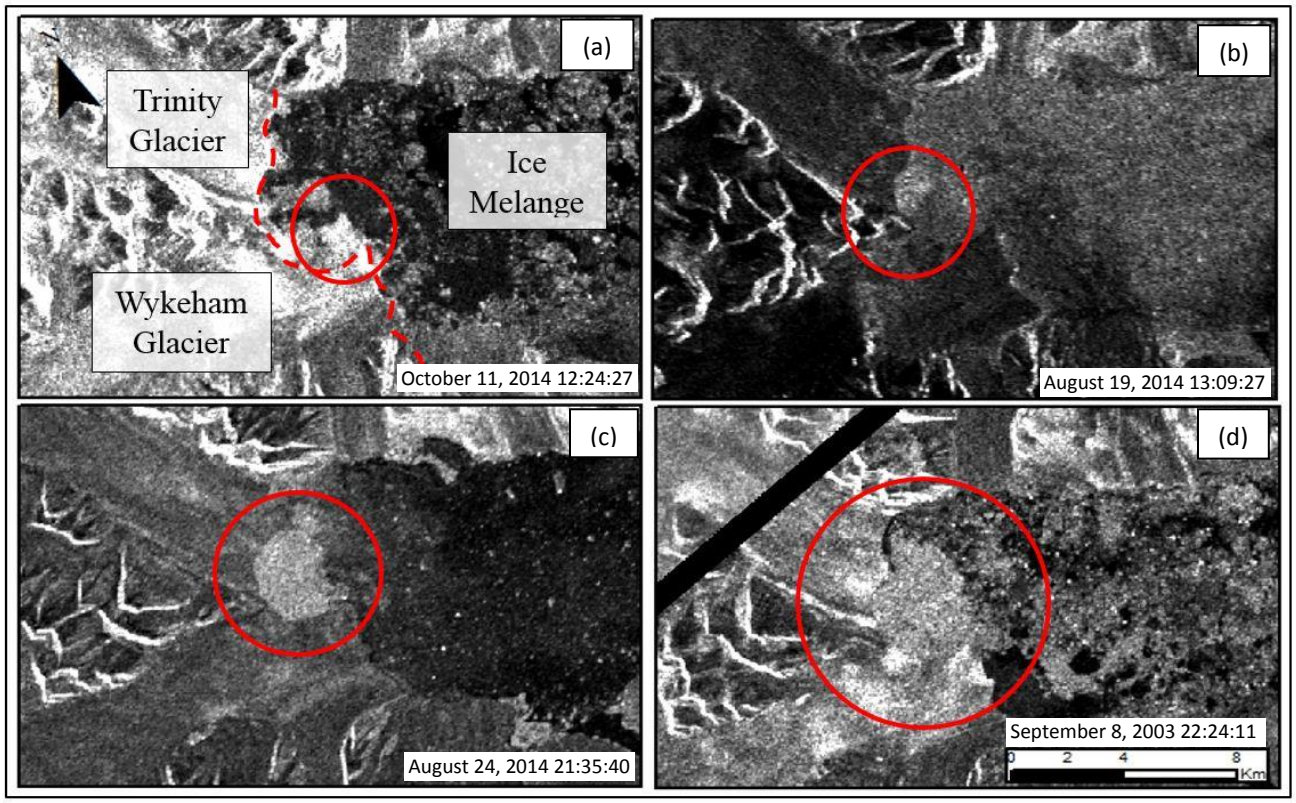

Figure 3.4: Examples of iceberg plume classification for Radarsat-2 ScanSAR Wide beam mode imagery (100 m resolution): (a) size 1 (<1 km^2); (b) size 2 (1-10 km^2); (c) size 3 (10-20 km^2); size 4 (>20 km^2). Dotted line shows the approximate terminus outline for Trinity and Wykeham Glaciers. Data and Products © MacDONALD, DETTWILER AND ASSOCIATES LTD (2015) – All Rights Reserved. RADARSAT is an official mark of the Canadian Space Agency.

Figure 3.5: Sea ice conditions at the terminus of Talbot Inlet: (a) approximate date of minimum sea ice extent with open water along entire terminus of Trinity Glacier; (b) approximate date of maximum sea ice extent showing the landfast ice mélange frozen along terminus of Trinity glacier.

Chapter 4: Results

4.1 Prince of Wales Icefield Plume Events

Of the 40 tidewater glaciers analyzed in this study, 25 were found to have produced at least one plume event between 1997 and 2015. The remaining 15 glaciers did not produce any detectable iceberg plumes during this time period, so are therefore not discussed any further (Table 4.1). The activity at the glaciers identified as being active is shown in Figures 4.2-4.6, with the timing and magnitude of plume events plotted in relation to the break up and freeze up dates of the surrounding sea ice. To provide a measure of the spatial distribution of plume activity, the glaciers were classified into those having produced 1-10 events, 11-50 events, 51-100 and 101-150 events, and are discussed further below and plotted in Figure 4.1.

It is worth noting that the availability of satellite imagery decreases outside of the summer season. For Radarsat, which was the primary source of imagery for this project, images from the CIS archive are available every 1-3 days during the summer and every 1-2 weeks during the rest of the year. Availability of imagery from year to year was also inconsistent, with some years having significantly more images available than others (Table 3.1). As a result, this could impact the number of iceberg plumes detected from between years as well as between seasons, as well as the number detected when sea ice was present and when it was not. There is a strong positive correlation between the number of detected iceberg plume events and the number of available satellite scenes in a given year (Figure 5.4). Known plume events were also likely undetected in many cases due to their size and the availability of imagery. It is not clear whether there was a decline in icebergs produced between 1997 and 2008 followed by an increase from 2009-2015, or if this simply reflects the availability of data. Since the availability of data and methods used to

detect iceberg plume events were the same for all glaciers in the study, the potential bias is consistent.

4.1.1 Plume Activity: 0-10 Events

The majority of the glaciers in this study produced few iceberg plume events over the 18 year time period. Out of the 25 glaciers identified as active, 16 of them only produced between 1 and 10 plumes between 1997 and 2015 (Figure 4.2). Most plume events occurred during the open water season (between approximately July and October), and some immediately prior to or following the open water season, with fewer events occurring when sea ice was present (Table 4.2). Only size 1 and size 2 plumes were produced by these glaciers, with the exception of South 4 Glacier which produced one size 3 event in 2014. Sea ice did not break out of the fiord in 1997 for several glaciers (South 6, Talbot, Unnamed 1, Unnamed 2, Unnamed 1 South, Cadogan 1, Cadogan 2, Cadogan 3 and Cadogan 5). No iceberg plume events were detected for any of the glaciers during this year.

4.1.2 Plume Activity: 11- 50 Events

Unnamed 1 South and Tanquary Glaciers were the most active in this group of glaciers. Unnamed South 1 Glacier (Figure 4.3c) produced most iceberg plumes between 2009 and 2015, the majority of which were size 1 in magnitude. Tanquary Glacier (Figure 4.3a) produced more plumes consistently over the time period, the majority of which were size 2. Most plume events were produced from these glaciers during the open water season. In the case of Unnamed 1 South Glacier (Figure 4.3b), many size 1 plume events were produced between 2008 and 2015 in the

month preceding the sea ice break up date. A similar pattern was not seen for Tanquary or Stygge Glaciers (Figure 4.3a and c).

4.1.3 Plume Activity: 51-100 Events

Two glaciers in the study produced between 51 and 100 plume events between 1997 and 2015 (Figure 4.4). South 2 and South 7 Glaciers are located on the southern coast of the POW. Both glaciers were actively producing iceberg plumes between about 1997 and 2003 (66 and 54 plumes, respectively). No icebergs plumes were identified for either glacier in 2004. A higher number of events were detected from South 2 Glacier from 2010 to 2015, including two size 3 plumes (Figure 4.4a). South 7 Glacier was less active between 2003 and 2006, but produced more and larger (more size 2) iceberg plumes between 2007 and 2015 (Figure 4.4b). Most plume events occurred during the open water season (between approximately July and October) and immediately prior to or following the open water season, with fewer events occurring when sea ice was present. During some years South 3 Glacier produced icebergs when sea ice was present (between approximately November and August), however these were restricted to smaller size 1 plumes compared to size 1, 2 and 3 plumes produced during the open water season.

4.1.4 Plume Activity: 101-150 Events

Cadogan and Ekblaw Glaciers produced 105 and 102 plumes, respectively, between 1997 and 2015. Both glaciers produced icebergs consistently over the 18 year time period. Cadogan Glacier (Figure 4.5a) produced size 1, 2 and 3 magnitude iceberg plumes while Ekblaw Glacier (Figure 4.5b) produced predominantly size 2 plumes. The size 3 plumes produced by Cadogan Glacier

appear to coincide with the timing of annual sea ice break up. Sea ice did not break out of the fiord in front of Cadogan Glacier in 1997 and no iceberg plume events were detected during that year. Similar to the other active glaciers in the study, most plume events for both glaciers occurred during the open water season (between approximately July and October) and immediately prior to or following the open water season, with fewer events occurring when sea ice was present. More size 1 plumes were detected from Cadogan Glacier when sea ice was present beginning around 2006.

Trinity and Wykeham Glaciers were found to be the most active iceberg plume producing glaciers in the study with 139 and 134 plumes detected, respectively (Figure 4.7). At Trinity Glacier, most of the plume events occurred during the open water season or immediately before or after it, with fewer events occurring when sea ice was present. Very few plume events were detected between January and June for all years, with the only winter events being seen in recent years (2013-2015). Most of the plumes produced by Trinity Glacier were size 1 or size 2 in magnitude (Figure 4.6a). Trinity Glacier produced the most size 3 plume events of all glaciers in the study with 11; these events occurred at least once per year between 1999 and 2006. Only one size 3 event was detected after 2006, when it was seen in 2012. One size 4 plume was also produced by Trinity Glacier in September 2003. The most plumes from Trinity Glacier were identified between 1999 and 2006 with fewer plumes detected between 2007 and 2010. The number of plumes detected increased again between 2011 and 2015.

Similar to Trinity Glacier, most of the iceberg plume events produced from Wykeham Glacier (Figure 4.6b) were detected during the open water season, although more events were detected than at Trinity when sea ice was present (approximately December to May) (Table 4.2). All of these events were smaller in size (size 1 or 2) compared to the events that occurred during the open

water season. Two size 3 events and one size 4 event were produced by Wykeham Glacier, but these were only detected in recent years, between 2011 and 2014. Sea ice did not break out of Talbot Inlet in 1997 and no iceberg plume events were detected from either Trinity or Wykeham Glaciers that year. About the same number of plume events are produced from Trinity and Wykeham Glaciers during the ~2-3 month open water season as occur during the rest of the year combined (Table 4.2).

Figure 4.7 shows the proportion of iceberg plume events for each year that were produced by Trinity and Wykeham Glaciers compared to all other glaciers from the study. With the exception of 1997 when no iceberg plumes were produced by either glacier, between approximately 20 and 60% of all icebergs for any given year were produced by Trinity and Wykeham.

Table 4.1: Total yearly detected plume events produced by all glaciers in the study between 1997 and 2015.

Glacier	Latitude	Longitude	1997	1998	1999	2000	2001	2002	2003	2004	2005	2006	2007	2008	2009	2010	2011	2012	2013	2014	2015	Total
Trinity	77.97	-78.57	0	8	9	9	6	7	13	4	6	6	0	4	5	2	10	12	7	12	19	139
Wykeham	77.89	-78.61	0	5	7	8	11	7	4	4	2	7	4	3	8	7	6	11	4	16	20	134
Cadogan	78.23	-76.94	0	5	7	8	3	3	4	6	9	8	5	2	6	5	10	6	5	4	9	105
Ekblaw	78.51	-76.71	3	10	8	6	5	6	4	6	3	6	2	3	3	4	7	9	5	6	6	102
South 2	77.33	-79.62	2	10	3	4	3	3	1	0	4	2	2	2	3	5	6	7	1	5	4	67
South 7	77.41	-78.76	3	2	1	5	0	5	0	0	2	1	4	1	5	4	5	5	4	5	2	54
Tanquary	78.46	-76.08	3	3	0	3	3	0	1	2	3	0	1	0	2	1	5	5	1	2	2	37
Unnamed 1 South	77.96	-77.94	0	1	0	0	3	1	0	0	1	1	0	1	4	2	3	3	0	3	4	28
Stygge	78.77	-78.24	0	0	2	0	0	0	1	0	2	0	0	0	1	0	1	0	1	2	1	11
Unnamed 1	77.98	-77.36	0	0	3	1	2	1	0	1	0	0	1	0	0	0	0	1	0	0	0	10
Cadogan 4	78.24	-76.70	1	0	0	1	0	0	0	0	0	1	0	0	0	0	4	0	1	0	0	8
Talbot	78.00	-78.24	0	1	0	1	1	0	2	0	1	0	1	0	0	0	0	0	0	0	0	7
Sands	78.95	-78.06	1	0	1	0	0	0	0	0	0	0	0	0	2	1	0	0	2	0	0	7
Bear	79.06	-78.62	0	0	0	0	0	0	0	2	2	0	0	0	1	2	0	0	0	0	0	7
South 6	77.38	-78.88	0	2	0	0	0	0	0	1	0	0	0	0	0	0	1	1	0	1	0	6
Hook	77.56	-81.60	1	2	1	0	0	0	0	0	0	0	0	0	0	0	0	0	0	0	0	4
South 4	77.33	-79.05	0	0	0	0	0	0	0	0	0	0	0	0	0	0	0	0	0	3	0	3
Palisade	77.39	-80.99	0	1	0	1	0	0	0	0	0	0	0	0	0	0	0	0	0	0	0	2
South 3	77.31	-80.30	0	0	0	0	0	0	0	0	0	0	0	0	0	0	1	0	1	0	0	2
Cadogan 1	78.04	-75.68	0	0	0	1	0	1	0	0	0	0	0	0	0	0	0	0	0	0	0	2
Alfred Newton	78.57	-74.89	0	0	0	0	0	0	0	0	0	0	0	0	0	0	0	0	2	0	0	2
Unnamed 2	77.91	-76.93	0	0	1	0	0	0	0	0	0	0	0	0	0	0	0	0	0	0	0	1
Cadogan 2	78.13	-75.72	0	0	0	0	1	0	0	0	0	0	0	0	0	0	0	0	0	0	0	1
Cadogan 5	78.24	-76.41	0	0	0	0	0	0	0	0	0	0	0	0	0	0	1	0	0	0	0	1
Leffert	78.69	-74.92	0	1	0	0	0	0	0	0	0	0	0	0	0	0	0	0	0	0	0	1
Easter 1	77.83	-77.93	0	0	0	0	0	0	0	0	0	0	0	0	0	0	0	0	0	0	0	0
Easter 2	77.81	-77.62	0	0	0	0	0	0	0	0	0	0	0	0	0	0	0	0	0	0	0	0
Easter 3	77.79	-77.68	0	0	0	0	0	0	0	0	0	0	0	0	0	0	0	0	0	0	0	0
Ekblaw 1	78.34	-75.09	0	0	0	0	0	0	0	0	0	0	0	0	0	0	0	0	0	0	0	0
Ekblaw 2	78.39	-75.28	0	0	0	0	0	0	0	0	0	0	0	0	0	0	0	0	0	0	0	0
Leffert North	78.77	-74.78	0	0	0	0	0	0	0	0	0	0	0	0	0	0	0	0	0	0	0	0
Leffert South	78.65	-74.82	0	0	0	0	0	0	0	0	0	0	0	0	0	0	0	0	0	0	0	0
Macmillan	78.52	-75.31	0	0	0	0	0	0	0	0	0	0	0	0	0	0	0	0	0	0	0	0
South 3	77.30	-80.29	0	0	0	0	0	0	0	0	0	0	0	0	0	0	0	0	0	0	0	0
South 8	77.38	-78.34	0	0	0	0	0	0	0	0	0	0	0	0	0	0	0	0	0	0	0	0
South Margin	77.56	-78.20	0	0	0	0	0	0	0	0	0	0	0	0	0	0	0	0	0	0	0	0
South Sands	78.85	-78.17	0	0	0	0	0	0	0	0	0	0	0	0	0	0	0	0	0	0	0	0
South Wykeham	77.78	-78.01	0	0	0	0	0	0	0	0	0	0	0	0	0	0	0	0	0	0	0	0
Unnamed North	79.00	-76.99	0	0	0	0	0	0	0	0	0	0	0	0	0	0	0	0	0	0	0	0
Wyville Thompson	78.41	-75.45	0	0	0	0	0	0	0	0	0	0	0	0	0	0	0	0	0	0	0	0
Total			14	51	43	48	38	34	30	26	35	32	20	16	40	33	60	60	34	59	67	741

Table 4.2: Distribution of total plume events for all glaciers in the study from 1997-2015 based on fiord sea ice conditions.

Glacier	Number (and %) of plume events when open water present	Number (and %) of plume events when sea ice present
Trinity	63 (46%)	74 (54%)
Wykeham	73 (53.7%)	63 (46.3%)
Cadogan	47 (44.8%)	58 (55.2%)
Ekblaw	58 (56.9%)	44 (43.1%)
South 2	32 (47.8%)	35 (52.2%)
South 7	30 (55.6%)	24 (44.4%)
Tanquary	18 (48.6%)	19 (51.4%)
Unnamed 1 South	8 (28.6%)	20 (71.4%)
Stygge	8 (72.7%)	3 (27.3%)
Unnamed 1	3 (30%)	7 (70%)
Cadogan 3	1 (12.5%)	7 (87.5%)
Talbot	3 (42.9%)	4 (57.1%)
Sands	2 (28.6%)	5 (71.4%)
Bear	2 (28.6%)	5 (71.4%)
South 6	3 (50%)	3 (50%)
Hook	0 (0%)	4 (100%)
South 4	0 (0%)	3 (100%)
Palisade	2 (100%)	0 (0%)
South 3	1 (50%)	1 (50%)
Cadogan 1	1 (50%)	1 (50%)
Alfred Newton	2 (100%)	0 (0%)
Unnamed 2	0 (0%)	1 (100%)
Cadogan 2	1 (100%)	0 (0%)
Cadogan 5	1 (100%)	0 (0%)
Leffert	0 (0%)	1 (100%)
Total	359	382

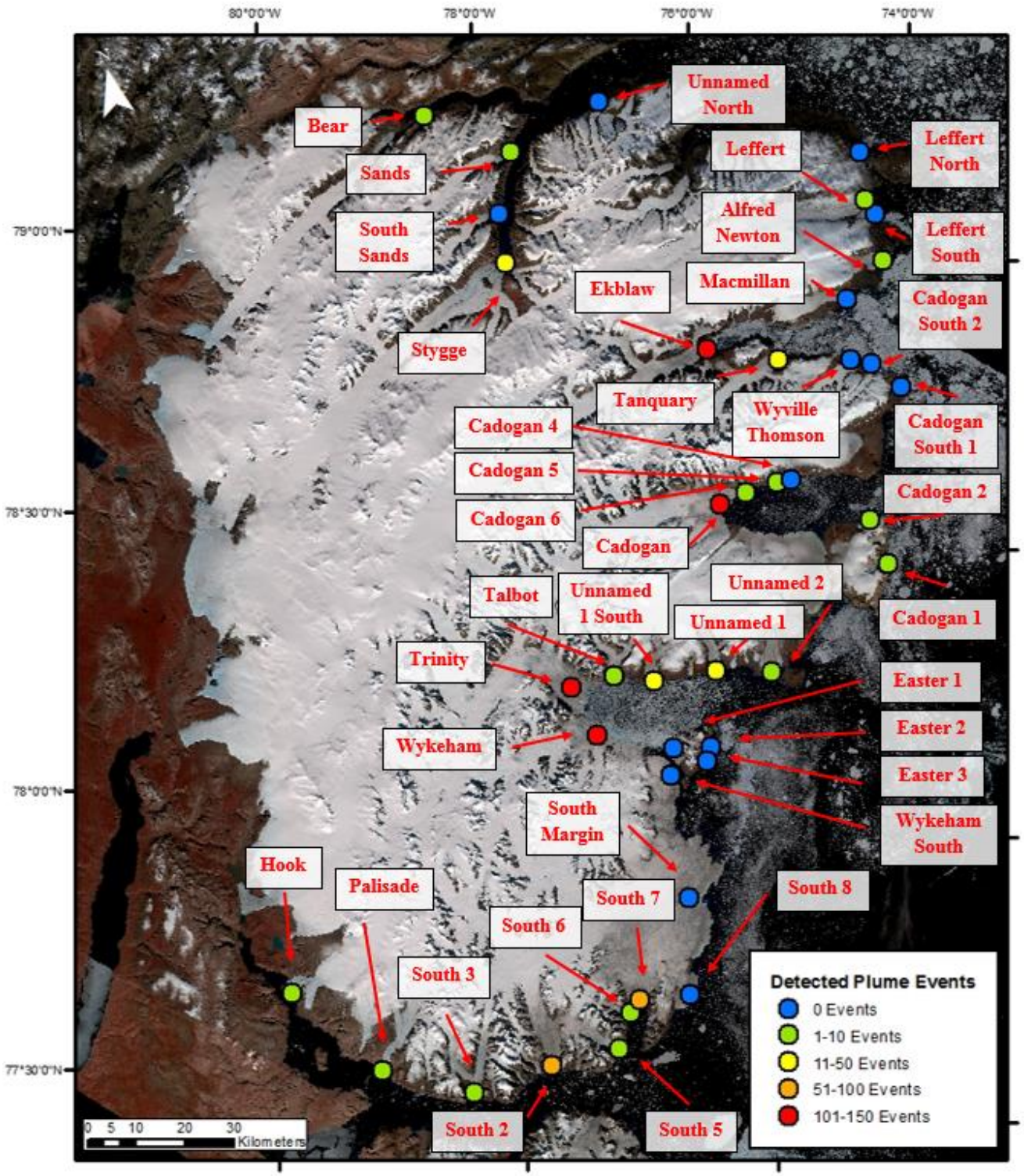

Figure 4.1: Distribution of cumulative plume events for all glaciers in the study area (tidewater, >1 km width) from 1997 to 2015. Base image: USGS/NASA Landsat-8 mosaic, July/August/September 2015.

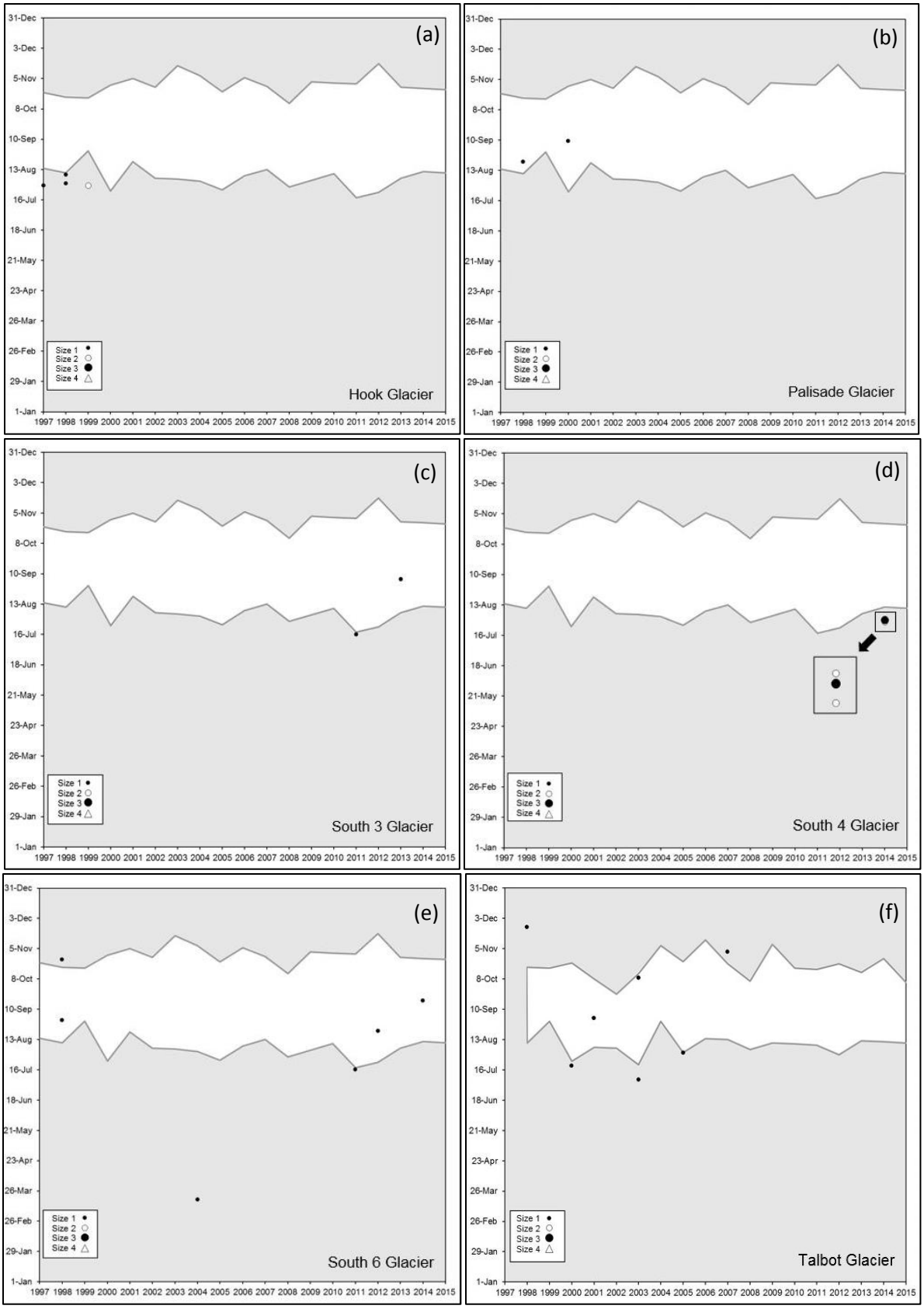
(a)
Hook Glacier
(b)
Palisade Glacier
(c)
South 3 Glacier
(d)
South 4 Glacier
(e)
South 6 Glacier
(f)
Talbot Glacier
Size 1
Size 2
Size 3
Size 4
31-Dec
3-Dec
5-Nov
8-Oct
10-Sep
13-Aug
16-Jul
18-Jun
21-May
23-Apr
26-Mar
26-Feb
29-Jan
1-Jan
1997 1998 1999 2000 2001 2002 2003 2004 2005 2006 2007 2008 2009 2010 2011 2012 2013 2014 2015

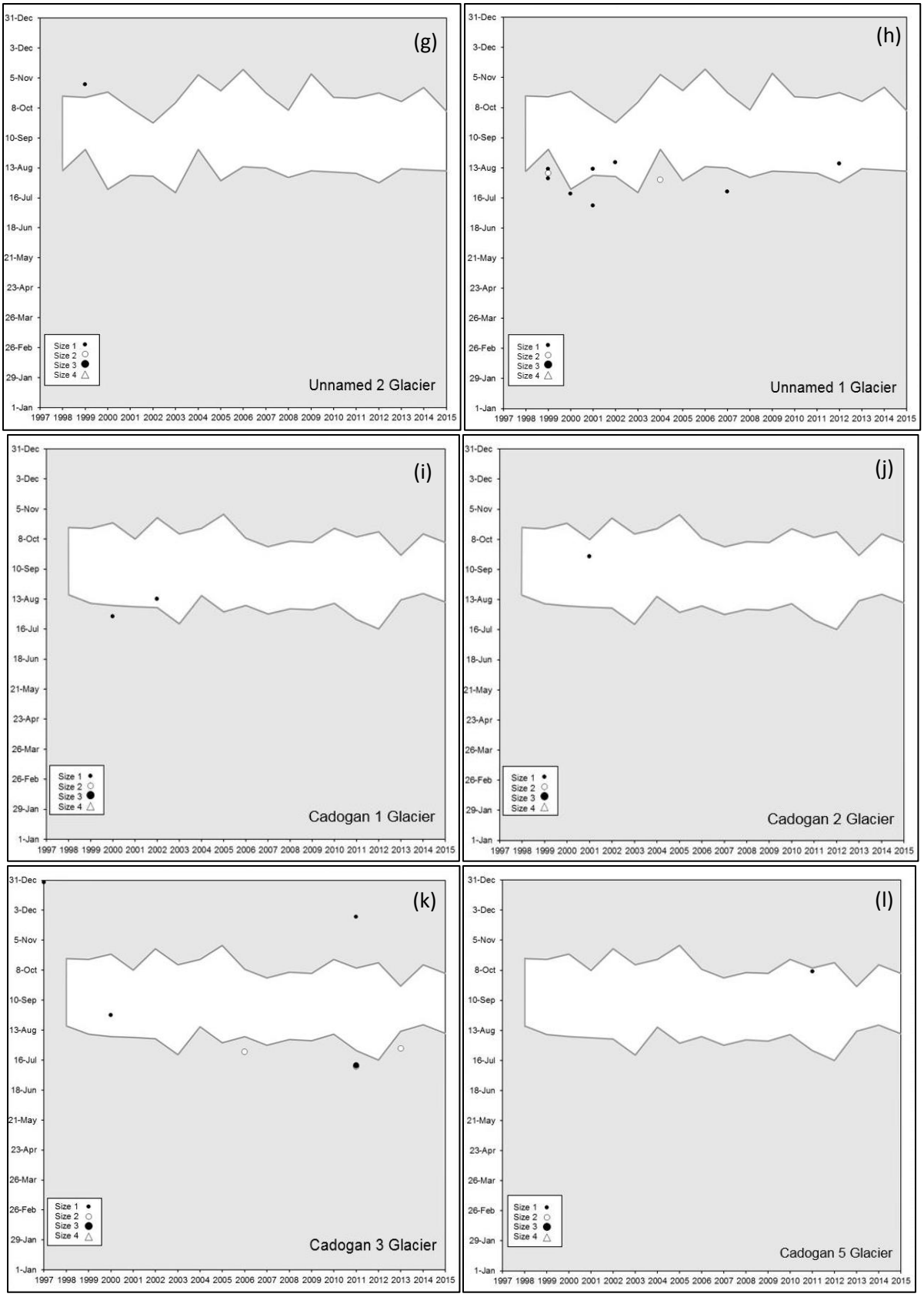
(g)
Unnamed 2 Glacier
(h)
Unnamed 1 Glacier
(i)
Cadogan 1 Glacier
(j)
Cadogan 2 Glacier
(k)
Cadogan 3 Glacier
(l)
Cadogan 5 Glacier
Size 1
Size 2
Size 3
Size 4
31-Dec
3-Dec
5-Nov
8-Oct
10-Sep
13-Aug
16-Jul
18-Jun
21-May
23-Apr
26-Mar
26-Feb
29-Jan
1-Jan
1997 1998 1999 2000 2001 2002 2003 2004 2005 2006 2007 2008 2009 2010 2011 2012 2013 2014 2015

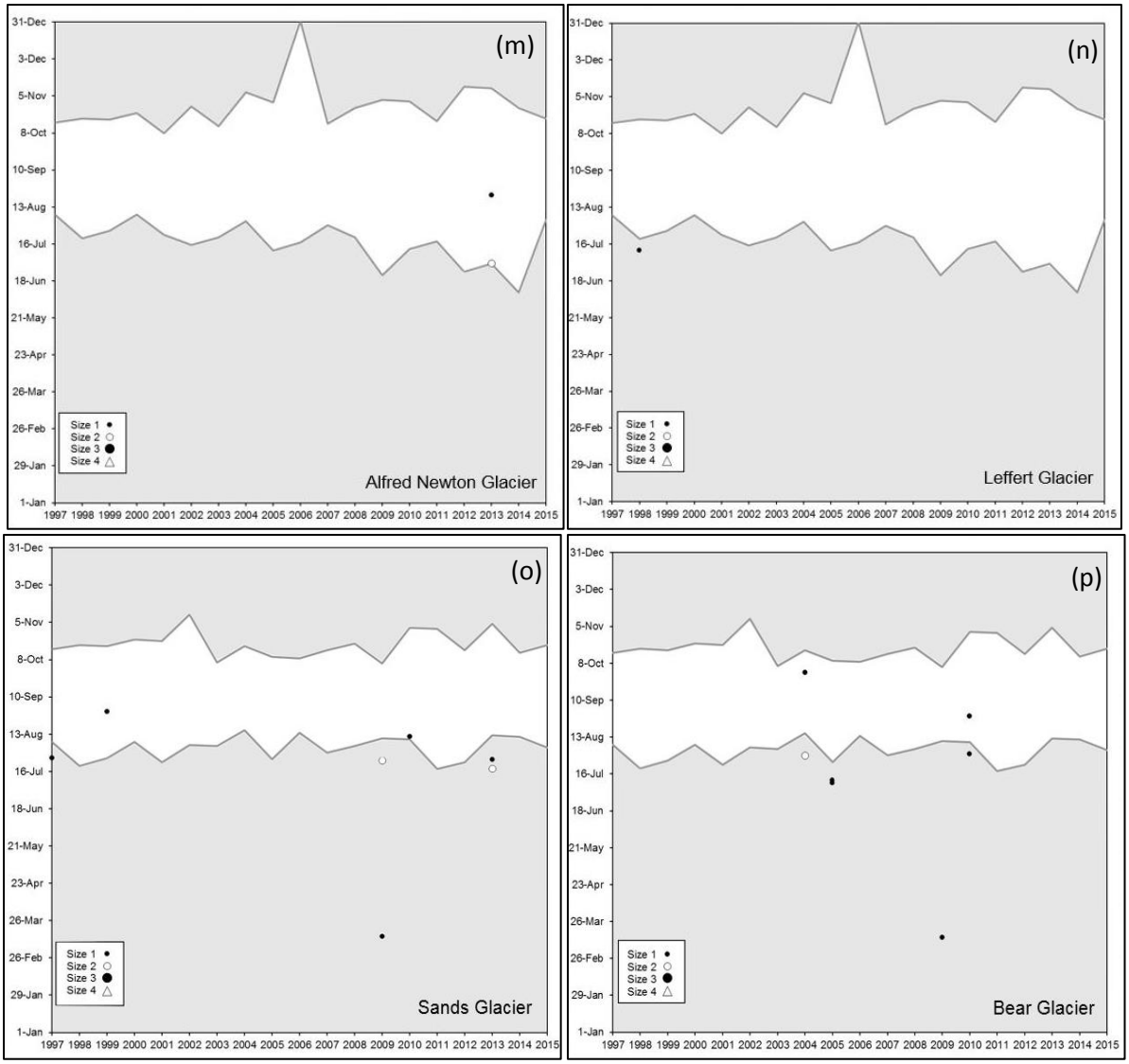

Figure 4.2: Temporal variability of iceberg plumes produced from glaciers (a-p) in the study that produced between 1 and 11 identifiable plumes between 1997 and 2015. Grey area represents the presence of landfast sea ice adjacent to the glacier terminus, and white area represents absence of landfast sea ice in this area. See Figure 4.1 for glacier locations.

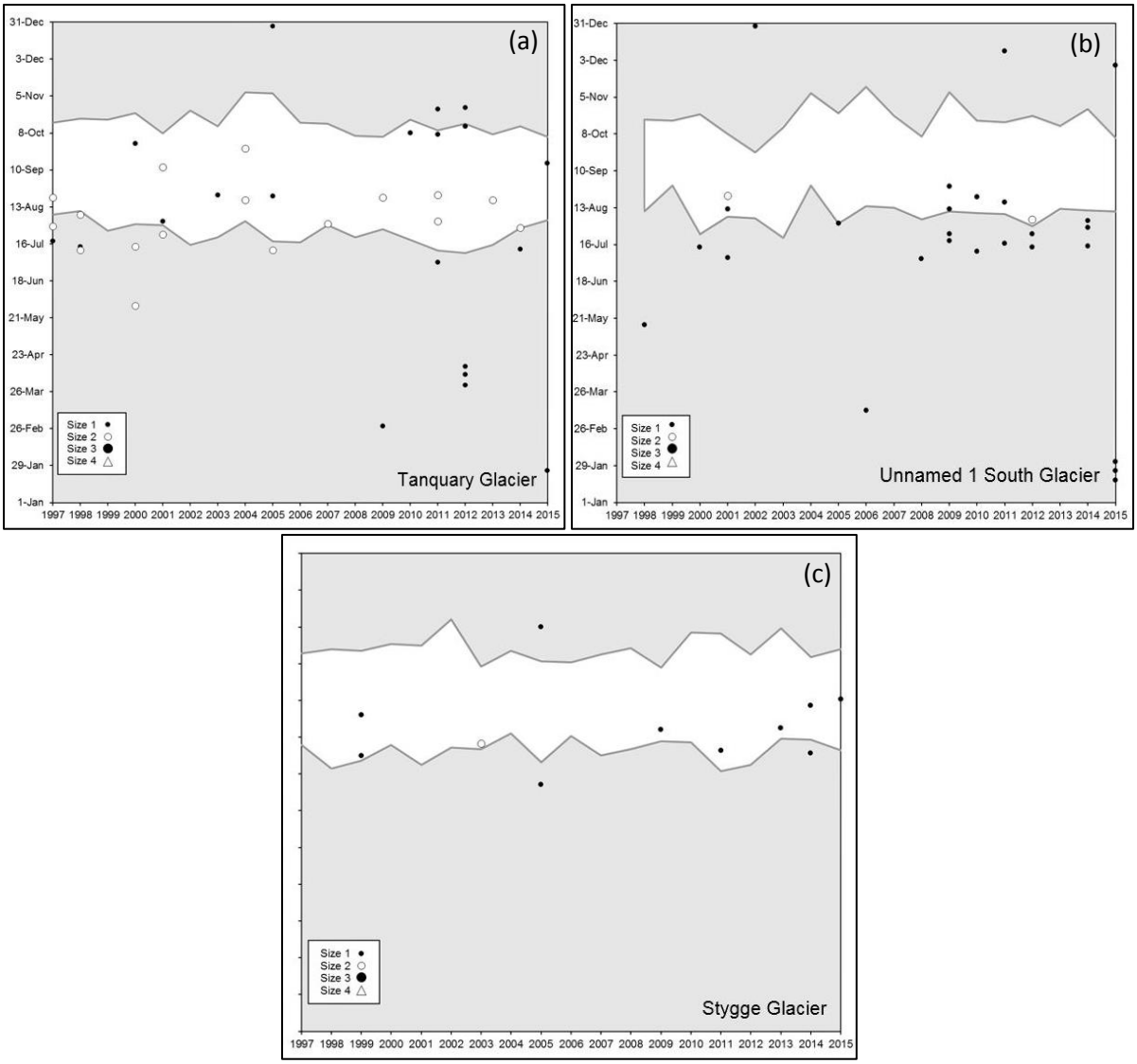

Figure 4.3: Temporal variability of iceberg plumes produced from glaciers (a-c) in the study that produced between 11 and 50 identifiable plumes between 1997 and 2015. Grey area represents the presence of landfast sea ice and white area represents absence of landfast sea ice.

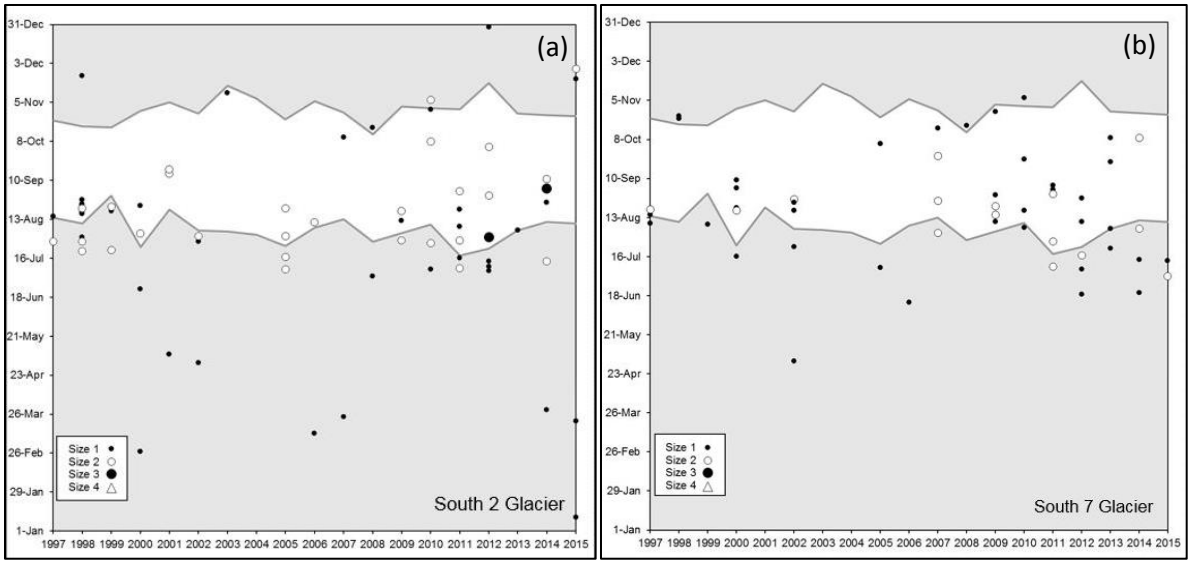

Figure 4.4: Temporal variability of iceberg plumes from (a) South 2 Glacier, and (b) South 7 Glacier, that produced between 51 and 100 identifiable plumes between 1997 and 2015. Grey area represents the presence of landfast sea ice and white area represents absence of landfast sea ice.

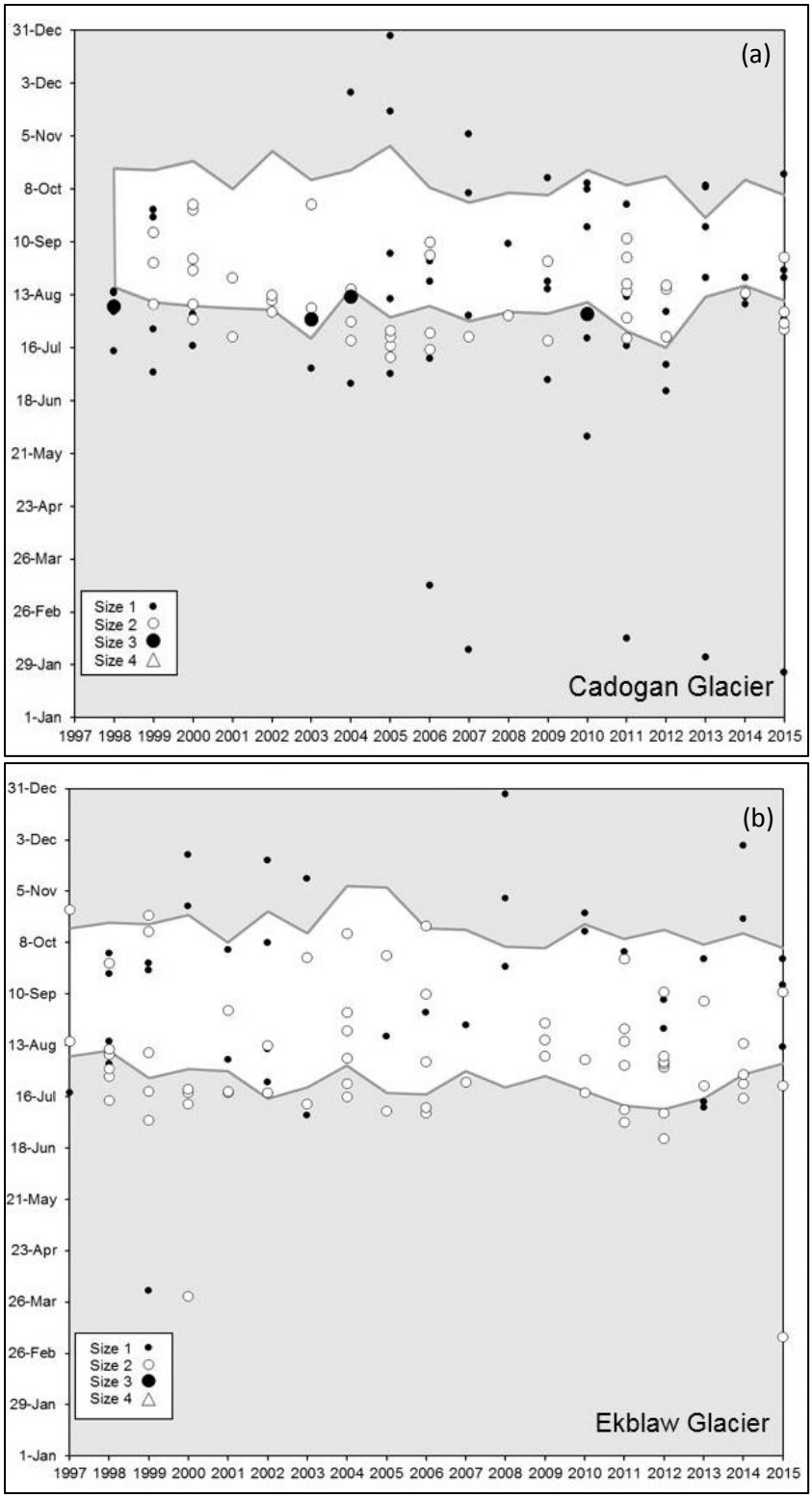

Figure 4.5: Temporal variability of iceberg plumes produced by (a) Cadogan Glacier and (b) Ekblaw Glacier between 1997 and 2015. Grey area represents the presence of landfast sea ice and white area represents absence of landfast sea ice.

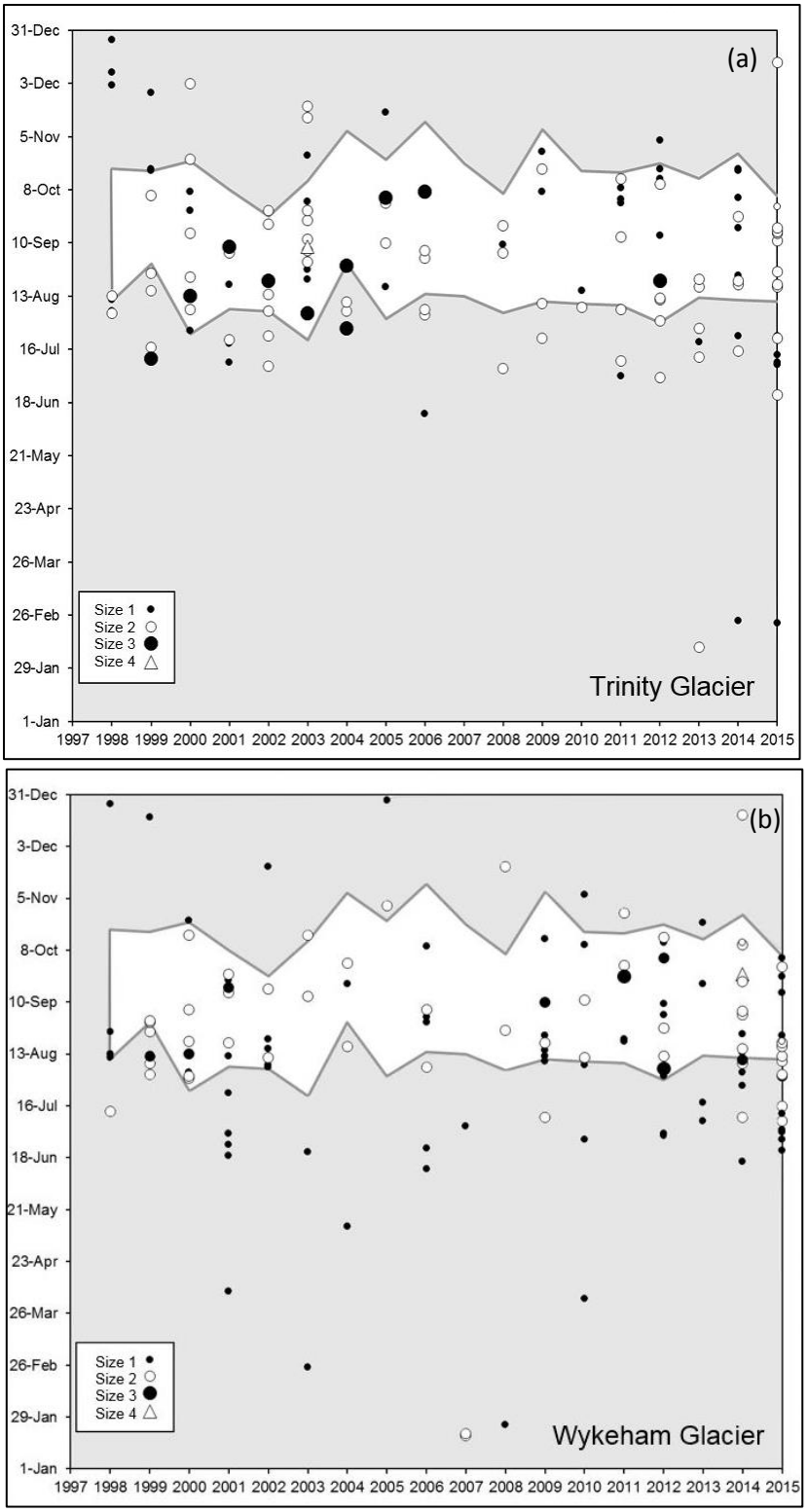

Figure 4.6: Temporal variability of iceberg plumes produced by (a) Trinity Glacier and (b) Wykeham Glacier between 1997 and 2015. Grey area represents the presence of landfast sea ice and white area represents absence of landfast sea ice.

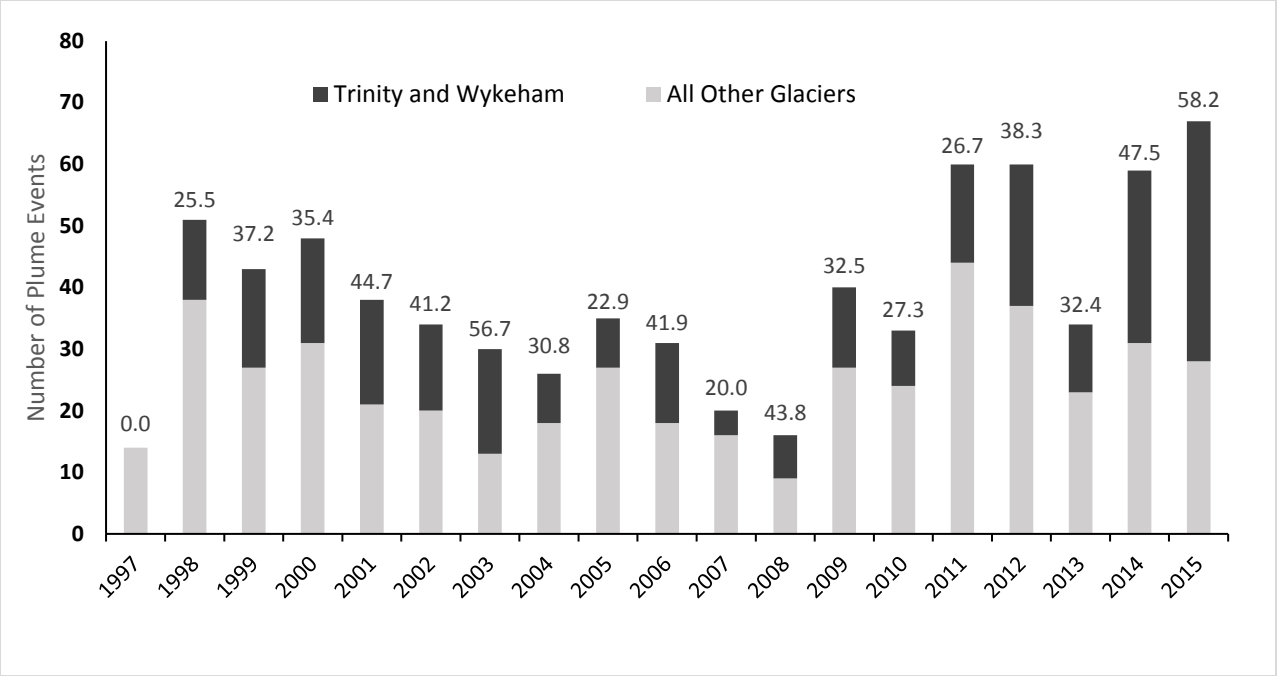

Figure 4.7: Total yearly plume events produced by Trinity and Wykeham Glaciers (dark grey) compared to plume events from all other major glaciers in the study (light grey). Figures above columns represent the proportion (%) of total iceberg plumes produced by Trinity and Wykeham Glaciers.

Chapter 5: Discussion

From the above descriptions, it is clear that there are marked variations in the number and size of iceberg plume events produced by the tidewater glaciers around POW, both over space and time. Trinity and Wykeham glaciers dominate the iceberg production process in this region, so these glaciers form a focus of the following discussion, although the patterns at other glaciers are also referenced where relevant. When assessing the causes and patterns of the observed iceberg plumes, there are two separate (but inter-related) questions that need to be addressed:

1. Why are some glaciers much more productive than others?
2. For a particular glacier, what controls the timing of iceberg production: both seasonally, and over the past 18 years?

These questions are addressed in the following sections.

5.1 Causes of Spatial Variability in Iceberg Production

5.1.1 Glacier Dynamics

Previous studies have found that the presence of sea ice at the terminus of a glacier can act to stabilize the calving front and allow for glacial advance to occur in the winter. In the summer when temperatures increase and sea ice begins to break out, the formation of meltwater on the surface of the glacier is able to permeate the surface through crevasses and increase glacier motion (Andersen et al., 2010; Vieli & Nick., 2011). As a result calving rate also increases, causing an increase in glacial terminus retreat (Howat et al., 2010, Amundson et al., 2010). A study completed by Van Wychen et al. (2016) on long-term trends in glacier velocity in the QEI show that only two

glaciers in the region, Trinity and Wykeham, have consistently accelerated between 1999 and 2015. These results are consistent with the findings of this study, which show that these two glaciers were the most active iceberg producing glaciers in the POW between 1997 and 2015.

For Trinity Glacier, Van Wychen et al. (2016) indicated that velocities increased from ~300-550 m a^{-1} in 1999-2002 to ~600-900 m a^{-1} from 2005 to 2008 (Figure 5.2). During this time period, Trinity Glacier was found to have been actively producing iceberg plumes, including many larger size 3 plumes, before appearing to decrease iceberg production beginning around 2007 (Figure 4.6a). This is consistent with a slight decrease in velocity between 2007 and 2008. The velocity of Trinity Glacier was found to have increased again, to ~800-1250 m a^{-1} in 2011 to 2015, with a slight decrease in velocity in 2013. These findings are also consistent with an increase in iceberg production during this time, including a drop in production during 2013.

Similar consistencies between iceberg plume events and velocity variations on Wykeham Glacier reported by Van Wychen et al. (2016) are also apparent. Velocities increased from ~250 m a^{-1} in 1999 to 2000, to ~350 m a^{-1} by 2004 to 2005, before decreasing to ~200 m a^{-1} by 2007-2008. Production of plume events during this time occurred consistently (though with less frequency than Trinity Glacier) from 1998 to 2004 before decreasing in frequency between 2005 and 2008, with the exception of 2006 when 7 plume events were detected (Figure 4.6b; Figure 5.2). The velocity of Wykeham Glacier then began to increase consistently to ~450 m a^{-1} between 2009 and 2015. This increase in velocity is consistent with a large increase in detected plume events from Wykeham Glacier between 2009 and 2015, including several size 3 and 4 events which had not been detected prior to 2011.

Although Trinity and Wykeham were the only glaciers identified by Van Wychen et al. (2016) to have consistently accelerated since 1999, they also identified Ekblaw Glacier as pulse type. This

means that Ekblaw Glacier underwent marked velocity variations along the lower 10 km of its length over the period 1999-2015, which correlates with the region of the glacier front where the glacier bed descends below sea level. This differs from the velocity variations observed on surge type glaciers, where the entire length of the glacier undergoes acceleration. Ekblaw Glacier was found by Van Wychen et al. (2016) to be decelerating between 2006 and 2015 from ~250 m a^{-1} to ~ 50 m a^{-1} but this study showed a consistent production of size 1 and 2 iceberg plumes between 1997 and 2015, with no clear decreasing trends over time (Figure 5.2).

The remaining active iceberg-producing glaciers identified in this study were found to have no significant velocity variations over the period 1999-2015 by Van Wychen et al. (2016). For example, glaciers identified in this study as being active in iceberg production such as Cadogan, South 2, South 7, Tanquary, Unnamed 1 South and Unnamed 1 had velocities between ~50 and 150 m a^{-1} (Van Wychen et al., 2014). Cadogan Glacier was found to consistently produce iceberg plumes between 1997 and 2015 and shows no clear trend in increasing or decreasing plume events throughout the time period. South 2, South 7 and Unnamed 1 South Glaciers show a small increase in iceberg production between approximately 2009 and 2015 despite no significant variations in velocity being observed during this time.

When all glaciers are considered together, there is no clear long-term trend in the annual number of iceberg plumes produced by the glaciers around POW over the period 1997 to 2015 (Figure 5.1). However, it does seem that the number of annual plumes can be divided into two main periods: a slight decrease over time between 1998 and 2008, following by a more productive period since 2009 with a general increase toward the present day. However, further research is required to understand whether this pattern is related to the availability of satellite imagery (Section 4.1), or to some kind of physical forcing.

As is seen in Figures 4.1 to 4.5, there is no clear spatial pattern around the POW showing a consistent increase or decrease in iceberg plume production between 1997 and 2015. Yet, through analysis of Trinity and Wykeham glaciers, there appears to be a broad correlation between glacier velocity and iceberg productivity which shows increases in glacier velocity coinciding with an increase in plume production and magnitude (Figure 4.6; Figure 5.2).

5.1.2 Terminus Retreat

Analysis of terminus outlines delineated for Trinity and Wykeham Glaciers periodically between 1959 and 1992, and annually between 1997 and 2015, show that Trinity underwent a total retreat of ~8.4 km during this time and Wykeham retreated by ~2.6 km (Figure 5.3). Annual terminus outlines were also delineated from 1997-2015 for the remaining plume-producing glaciers in Talbot Inlet (Unnamed 1 South, Unnamed 1 and Unnamed 2 Glaciers; Figure 5.3). Each of these glaciers each underwent a terminus retreat of about 1km.

For Trinity Glacier, between 1997 and 2002 there was little change in the terminus position. The north side of the terminus showed a small retreat in position while the south side showed a slight advance during this time period. This can likely be attributed to seasonal patterns of advance and retreat of the glacier, where the terminus advances slightly in the winter and retreats in the summer. From 2003 to 2007, the terminus consistently retreated between approximately 400 and 600 m per year. The most significant yearly retreat occurred between 2011 and 2012 where the south side of the terminus retreated approximately 1 km, disconnecting the shared terminus of Trinity and Wykeham Glaciers. No significant changes were observed between 2013 and 2015, where the amount of retreat ranged between about 0 and 400 m.

Wykeham Glacier underwent less overall retreat compared to Trinity Glacier. Between 1997 and 2009 terminus position for the entire glacier width was variable, with slight advance some years and slight retreat during others. During 2010 and 2011, more significant retreat of around 800 m was seen on the north side of the terminus, near Trinity Glacier, with little change on the south side. Up until 2012, Trinity and Wykeham Glaciers shared a terminus. The ~1 km retreat observed at Trinity Glacier between 2011 and 2012 was also seen at Wykeham Glacier, separating them from each other. Gradual terminus retreat occurred between 2012 and 2015 and was variable, ranging between about 0 and 600 m. The south side of Wykeham Glacier near South Wykeham Glacier has not undergone significant retreat compared to the once-shared terminus with Trinity Glacier.

Between 1997 and 2003, Talbot Glacier fed into Trinity Glacier from the north and therefore did not have a separate terminus. From 2003 onward, the terminus retreat of Talbot Glacier was gradual and varied between about 0 and 100 m per year during this time. For Unnamed 1 South, Unnamed 1 and Unnamed 2 Glaciers, terminus positions were variable between 1997 and 2006 before beginning a gradual retreat between 2007 and 2015.

Trinity and Wykeham Glaciers underwent the most significant retreat of all glaciers in the POW between 1959 and 2015. When compared to the timing of plume events found by this study, there is no clear correlation between years of gradual retreat and an increase in plume events over the same time period. There is also no clear correlation between years with significant retreat (2011-2012) and an increase in plume events. However, these findings are consistent with the velocity increases found by Van Wychen et al. (2016). This implies that plume events from these glaciers are likely primarily driven by ice moving through the terminus as opposed to terminus retreat.

5.2 Causes of Temporal Variability in Iceberg Production

5.2.1 Sea Ice Patterns

Previous studies have suggested that there is a strong relationship between the presence of sea ice at the terminus of a glacier and the stability of the calving front (Reeh et al., 2001; Herdes et al., 2012; Pope et al., 2012; Carr et al., 2013). Fast ice that forms at the terminus of the glacier can act as a barrier between the calving front and the open ocean. Major calving events and loss of floating ice tongues have been found to occur after the break-up of this ice buffer from the terminus (Reeh et al., 2012). The tightly packed mix of sea ice and icebergs located at the terminus of tidewater glaciers during the fast ice season is known as the ice mélange. The ice mélange has also been found to have a stabilizing effect on the terminus of tidewater glaciers by acting as a barrier and preventing calving (Joughin et al., 2008; Amundson et al., 2010; Howat et al., 2010 Moon et al., 2015).

In this study it was found that landfast sea ice typically broke apart at each glacier every year, with break-up dates usually occurring between July and August and freeze-up dates between October and November (Figures 4.2 to 4.6). A major exception was for 1997, when sea ice did not break out in front of the glaciers in Talbot Inlet or those immediately surrounding Cadogan Glacier (Figures 4.5 and 4.6). One exception to the typical freeze-up dates was for Leffert and Alfred Newton Glaciers (located on the NE POW), where for the 2006 season, sea ice did not become landfast until January 1, 2007 (Figure 4.2m and n). These two glaciers also display a pattern of sea ice break-up date becoming progressively earlier between 1997 and 2014, while the freeze-up date remained relatively constant.

5.2.2 Presence of Landfast Sea Ice at Glacier Termini

The plume analysis from 1997 to 2015 indicates that a clear relationship exists between the presence of sea ice at the termini of tidewater glaciers around POW and the production of iceberg plumes. For all glaciers in the study, plume events occurred mostly during the open water season, immediately prior to the breakup of landfast ice or immediately following the formation of landfast ice. However, several events did also occur when sea ice was present at the terminus, including the midwinter. It was found that after landfast sea ice had broken up in the fiord and the ice mélange was able to drift away from the glacier termini that more plume events were detected. This was especially clear with the most active glaciers in the study, Trinity, Wykeham, Cadogan and Ekblaw Glaciers (Figures 4.5-4.8). Events occurring immediately prior to the open water season are likely a result of warming air and ocean temperatures in the late spring and summer. This can result in thinning of sea ice in the fiord and the formation of meltwater ponds on the surface, decreasing its stability. Conversely, shortly after the formation of landfast sea ice in the fall there is little to no ice mélange formed at the termini of the glaciers that would provide any significant stability for it. This is likely a contributing factor for the occurrence of iceberg plumes soon after the formation of fast ice.

Between 1997 and 2015, Trinity Glacier produced 63 iceberg plumes during the ~2-3 month open water season compared to 74 events when landfast sea ice was present during the remaining ~9-10 months of the year. Similar values were seen for Wykeham Glacier with 73 plumes produced during the open water season and 63 when sea ice was present (Table 4.2). Most of the iceberg plume events produced by glaciers in the study were size 1 and 2 in magnitude and occurred predominantly during the open water season. Of the plumes that were produced when sea ice was

present, most were size 1 or 2 in magnitude. The larger size 3 and 4 plumes were found to be primarily produced during the open water season with few exceptions (Figure 5.5).

The findings of this study that far fewer calving events occurred when landfast sea ice was present is consistent with the results of Herdes et al. (2012), who found similar patterns for Belcher and Fitzroy glaciers on Devon Island. Pimentel et al. (2017) explored the effects of backstress produced by the presence of sea ice and an ice melange at the terminus of Belcher Glacier. They found that a decrease in this backstress could be responsible for steady increases in velocity recorded at a lower GPS station near the terminus. The velocity returns to average in October once sea ice has formed at the terminus. However, since calving events still occurred while landfast sea ice was present for Belcher and POW glaciers studied here, it is likely that other contributing factors are also important. These are evaluated further below.

5.2.3 Oceanic Conditions

CMEMS TOPAZ4 oceanic temperature model data shows that between 1959-2009 mean temperature for the POW (ranging from approximately 77 to 79 °N) and surrounding waters in the QEI did not change significantly to a depth of 400m (Figure 5.6). Around the POW, bed depth of tidewater glaciers does not extend >400m below sea level, so ocean temperature changes at depths below this were not considered (Van Wychen et al., 2016). Mean annual water temperatures at all depths do not rise above 0°C within the POW throughout this time period. Based on the studies of Motyka et al. (2011) and O'Leary & Christofferson (2013) in Greenland, it might be expected that warmer waters at depths of around 200-300 m could cause basal erosion at the termini of POW glaciers leading to decreased stability and increased calving. Data for the region showed only small

changes in temperature between 50 and 200m depth for waters surrounding the POW, but the mean temperature at these depths did not rise above 0°C and would therefore likely not cause significant basal erosion. However, due to the lack of long term ocean temperature measurements taken near the termini of each of these glaciers, and the potential inability for a large-scale ocean model to correctly downscale to single fiords, it cannot be said definitively that variations in local ocean temperatures are not impacting iceberg production.

5.2.4 Tidal Conditions

Modelled tidal data from WWW Tide/Current Predictor was analysed for a 5 year period from 2011-2015 to identify whether patterns exist between the rise and fall of daily or monthly tidal cycles and iceberg plume events from Trinity and Wykeham Glaciers (Figure 5.7). Analysis of this tidal data shows no clear relationship between the timing of spring and neap tides and the production of icebergs from these glaciers. Iceberg plume events appear to occur during both spring and neap tidal periods, as well as during periods in between, with no clear consistency. Another factor which supports the lack of a tidal connection to the calving of these glaciers is that they do not always produce iceberg plumes on the same day, even though they are adjacent to each other and therefore under the same tidal influence.

Given that the tidal data is at a low spatial resolution that would not vary between glaciers in the POW, it is expected that results would be similar for the remaining glaciers in the study. The availability of smaller temporal and spatial scale observational data for this region could account for the lack of relationship detected between tidal cycles and glacier plume events and should be investigated further if possible. For example, this could be achieved through the use of water

pressure sensors and hourly time-lapse photography to monitor with higher accuracy the timing of tidal conditions directly at the terminus of POW glaciers, while also capturing plume events of varying sizes.

5.2.5 Atmospheric Conditions

Mean surface air temperatures from June to September for 1997-2015 using NCEP reanalysis data were plotted to determine whether temperatures have changed during the summer melt (and open water) season over the study period and if this coincides with timing and frequency of iceberg production (Figure 5.8). This reanalysis data is based on a 1981-2010 climatology. Results show a general increase in mean June to September temperatures from 1997 to 2015 at a rate of about 0.7°C decade^{-1} with low statistical significance.

Seasonal surface air temperature anomalies based on the 1981-2010 climatology were plotted for each year from 1997-2015 to identify whether there were any spatial connections between anomalous years in the POW region and the production of icebergs (Figure 5.9). Results show above average temperatures for most years between 1997 and 2015, with temperatures ranging from +0.3°C in 1998 to +2.6°C in 2012. Temperatures were below average in 1997 and 2013 by between -0.6°C and -1.2°C.

These findings indicate that summer air temperatures in the POW region have generally warming between 1999 and 2015, with the exception of a few anomalously cold years such as 2013 (Figure 5.8). Previous studies have found that increased surface ablation caused by warming air temperatures can lead to more percolation of surface melt to the bed of the glacier, increasing basal sliding (Howat et al., 2010). Higher rates of movement can cause more crevasses to form on the

surface of the glacier, both of which can contribute to increased rates of ice being discharged through calving (Vieli & Nick, 2011). When compared to the total number of iceberg plumes detected for all glaciers in the study from 1997-2015 (Figure 5.1), a weak positive correlation exists (Figure 5.9).

A decrease in mean seasonal surface air temperatures in 2013 to -2.7°C from 1.4°C the previous year coincide with a drop in total identified plume events for the same year from around 60 events to 34. It is possible that there is a relationship between these patterns, although previous years where mean seasonal temperatures were below average (2004, 2006 and 2014) do not appear to coincide with years of lower than average detected plume events.

Looking at Trinity Glacier during 2012, an anomalously warm year, 12 plumes were detected, 11 of which were size 1 or 2. All but 2 of these events occurred during the open water season. Compared to 2013, which was an anomalously cold year, only 7 events were detected (all size 1 and 2), the lowest annual total between 2011 and 2015. A similar decrease in detected plumes occurred for Wykeham Glacier from 11 in 2012 to 4 in 2013. The same was not found for Cadogan and Ekblaw glaciers, the other two most active in the study, which remained consistently productive between these years. Since Trinity and Wykeham glaciers are responsible for a large portion of the icebergs produced from the POW (38.3% in 2012 and 32.4% in 2013), any significant changes in plumes detected from these glaciers will impact the total number of plumes detected from all glaciers in that year.

Locally measured observational data and a consistent dataset of SAR imagery would be more accurate in determining if there is a clear relationship between timing of plume events from individual glaciers and variations in surface air temperature (Figure 5.4).

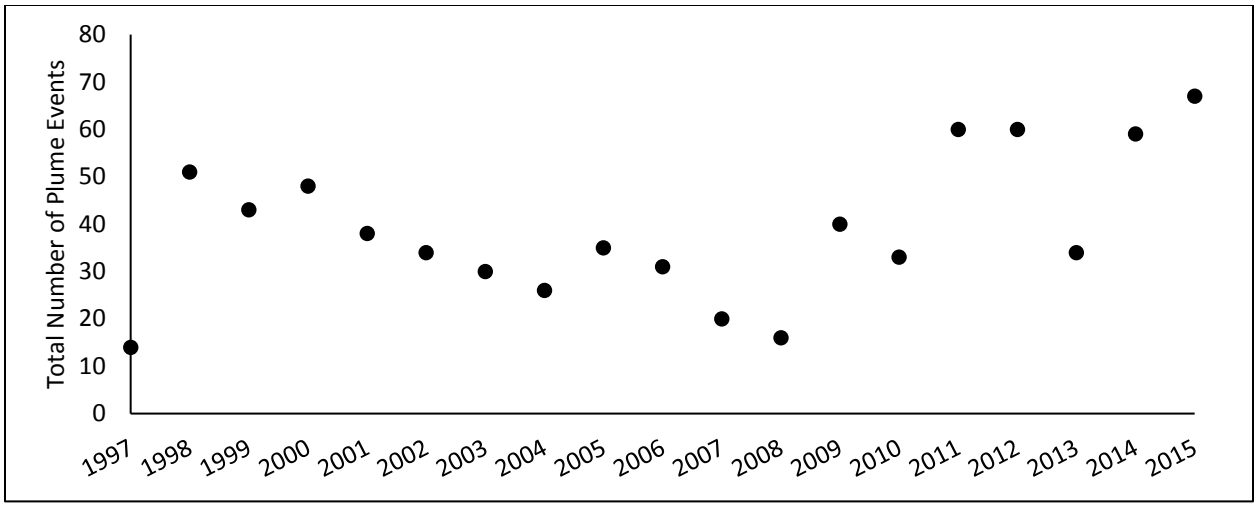

Figure 5.1: Temporal distribution of total plumes by year for all major glaciers in the study from 1997 to 2015.

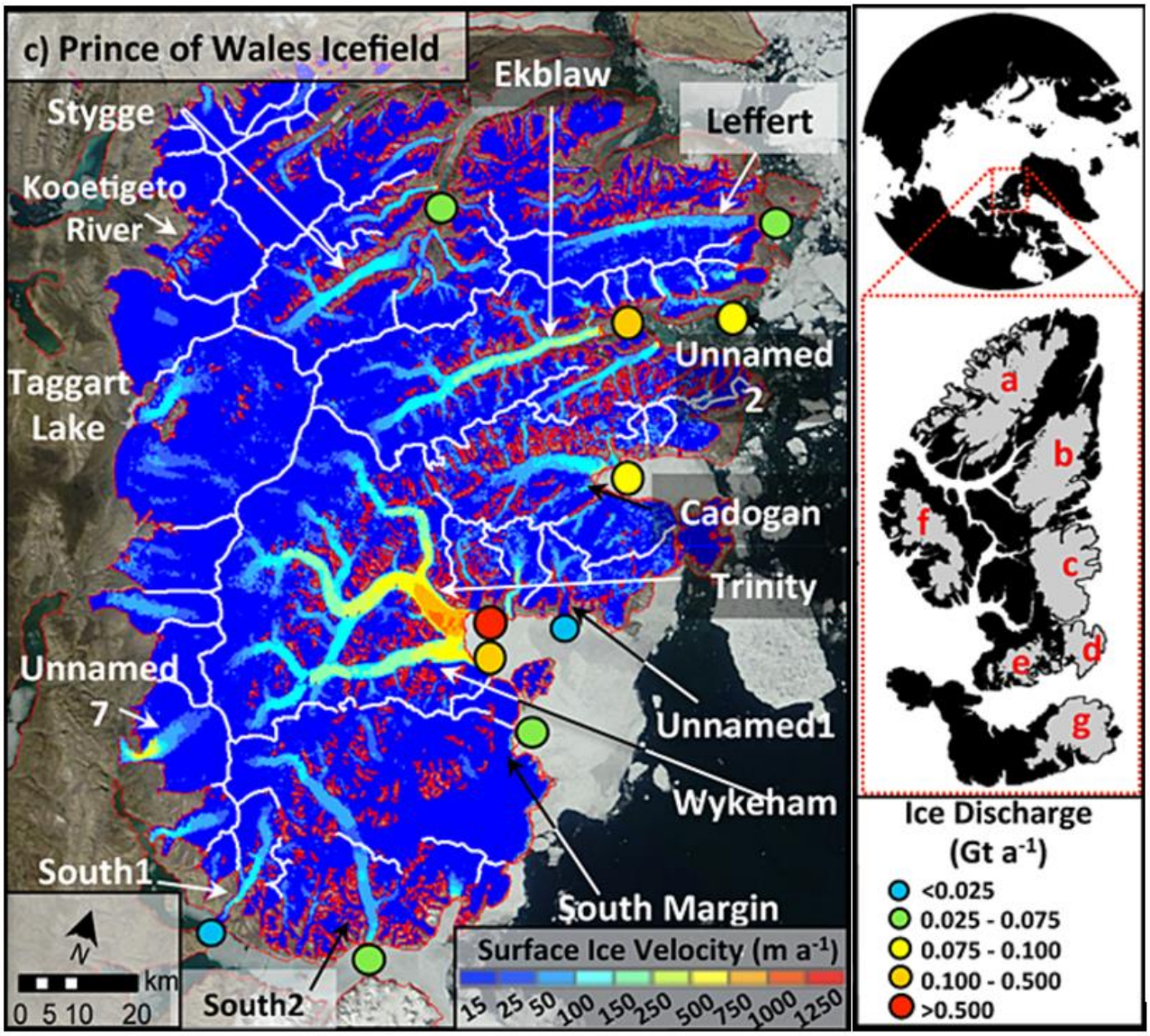

Figure 5.2: Surface velocity and ice discharge map for the Prince of Wales Icefield. (base image: Moderate Resolution Imaging Spectroradiometer, 4 July 2011). Inset map: study site. Reproduced from Van Wychen et al., 2014. Copyright 2014, with permission from the American Geophysical Union (AGU)

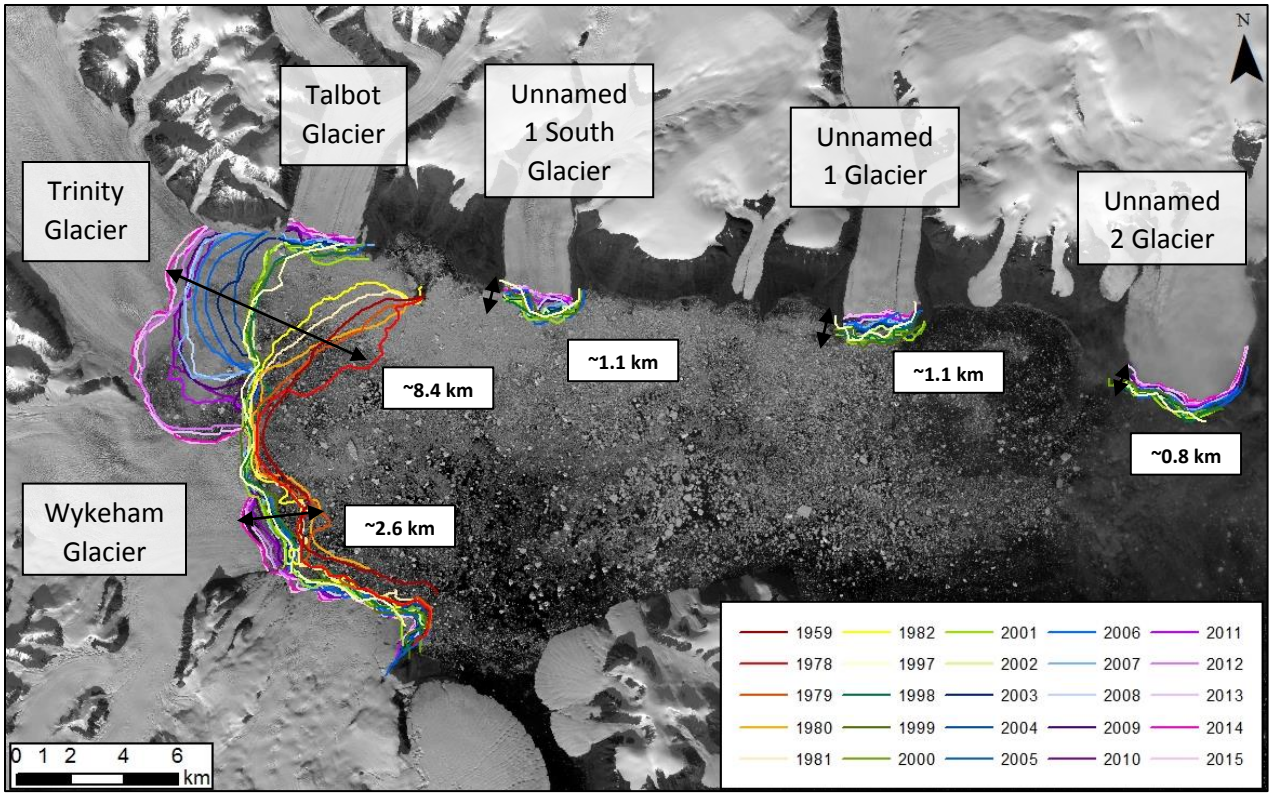

Figure 5.3: Terminus outlines 1959-2015 for Trinity and Wykeham glaciers and 1997-2015 for Talbot, Unnamed 1 South, Unnamed 1 and Unnamed 2 Glaciers in Talbot Inlet. Base image: USGS/NASA Landsat August 29, 2014.

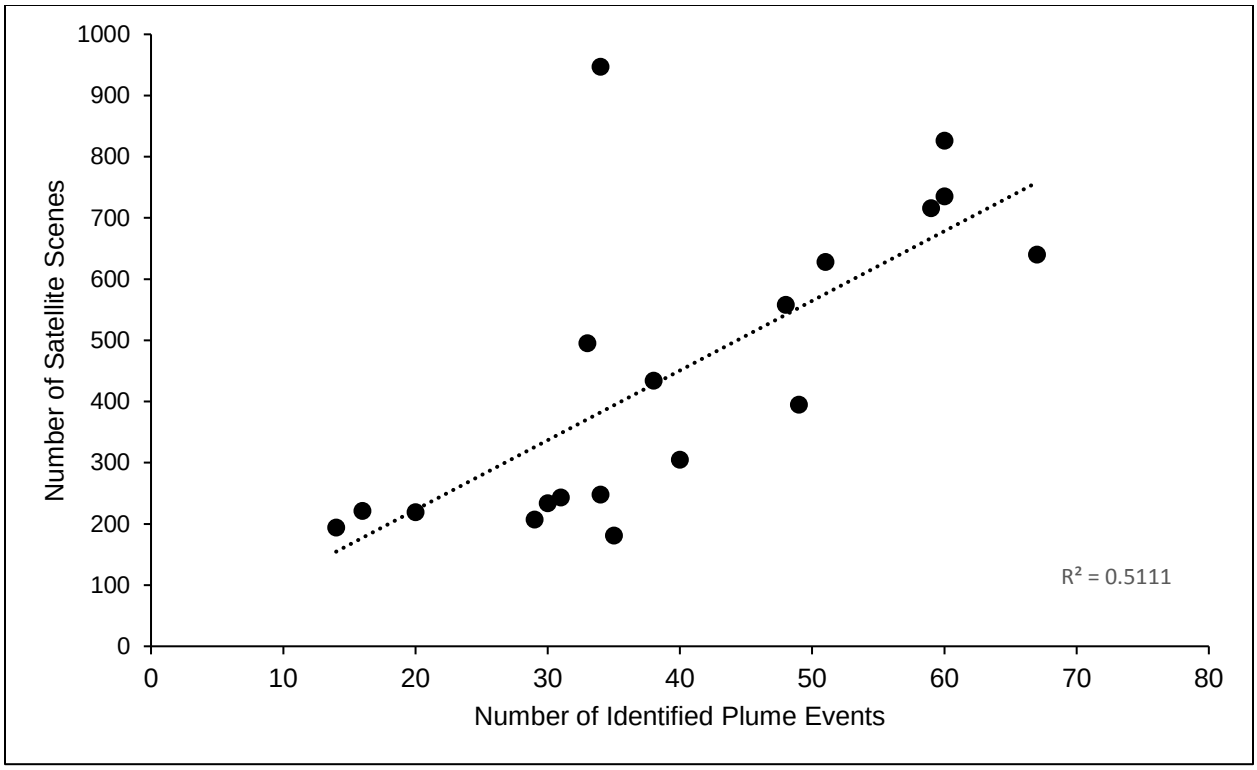

Figure 5.4: Total yearly plume events produced by all major glaciers in the study compared to the number of satellite scenes analysed for each year.

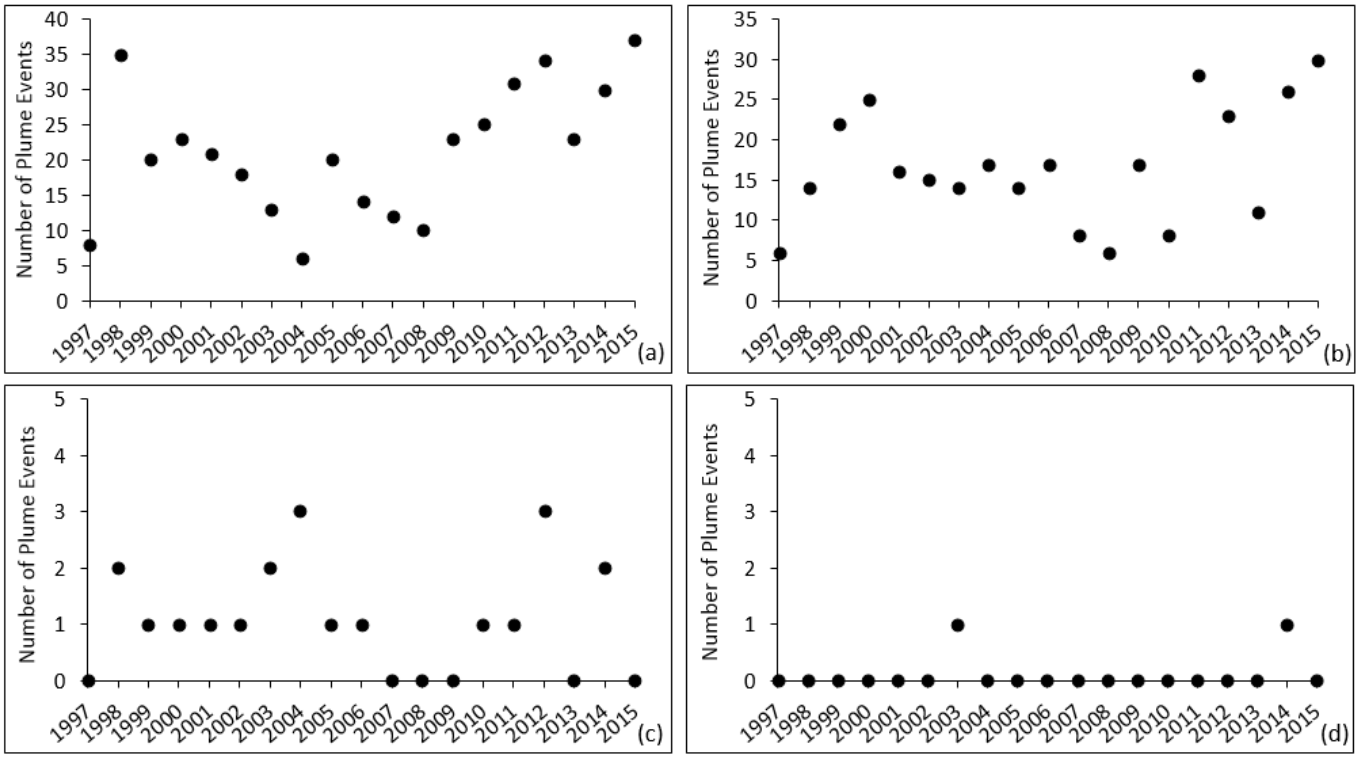

Figure 5.5: Temporal distribution of total yearly iceberg plumes for all major glaciers in the study by size: (a) size 1 plumes; (b) size 2; (c) size 3; (d) size 4.

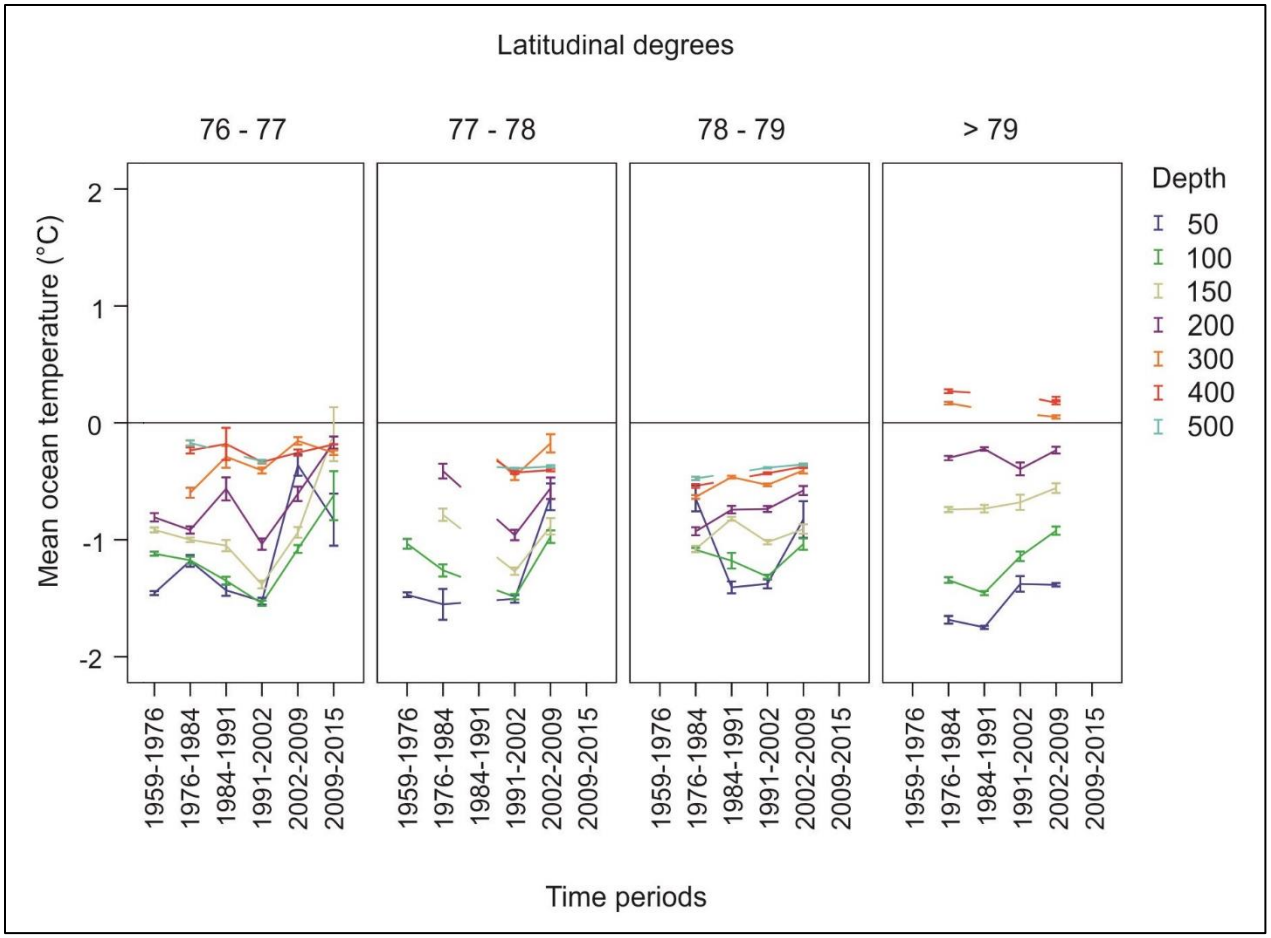

Figure 5.6: CMEMS TOPAZ4 modelled mean oceanic temperature data from 1959-2015 for the QEI for 50-500m depths. Source: A. Cook, personal communication, August 18, 2017

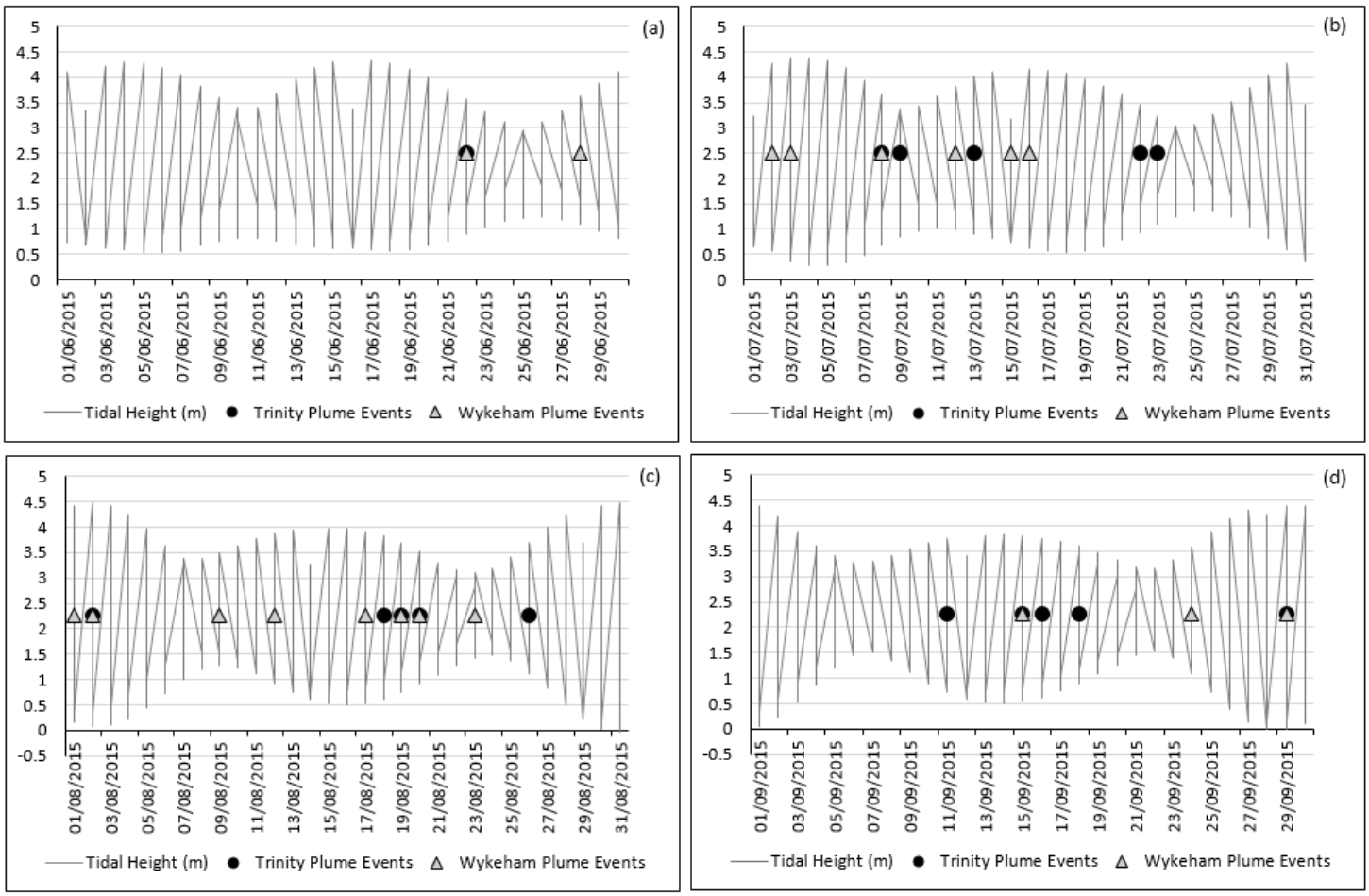

Figure 5.7: Daily tidal heights for (a) June, (b) July, (c) August and (d) September compared to timing of iceberg plume events produced from Trinity and Wykeham glaciers.

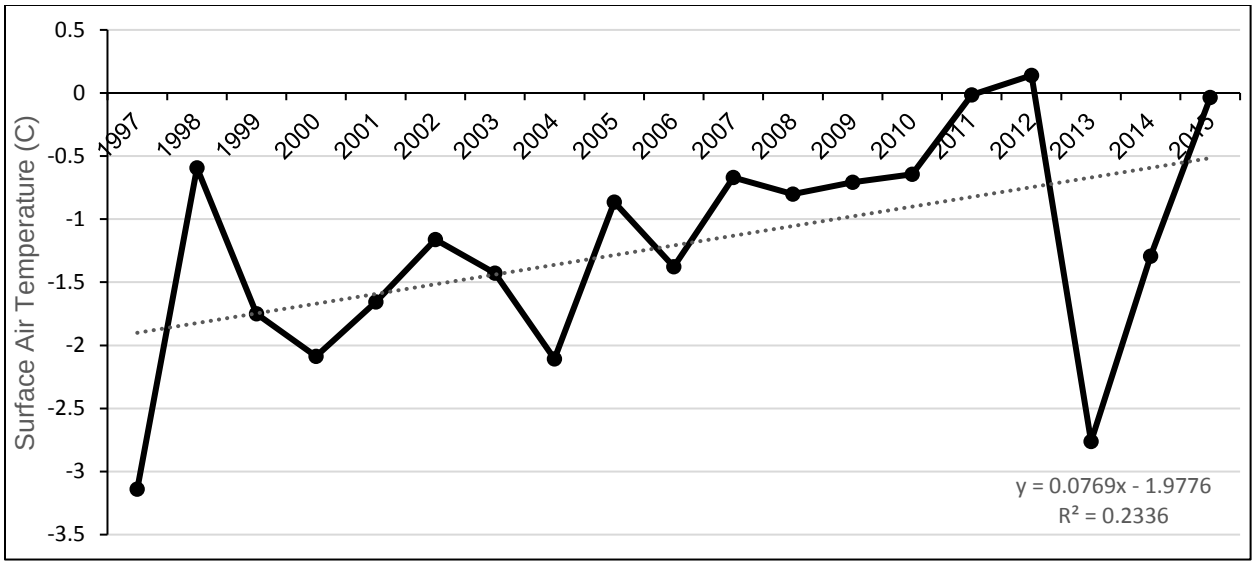

Figure 5.8: NCEP Reanalysis surface air temperature seasonal climate composite using 1981-2010 climatology for June to September from 1997-2015 for the Prince of Wales Icefield. Source: Kalnay et al., 1996

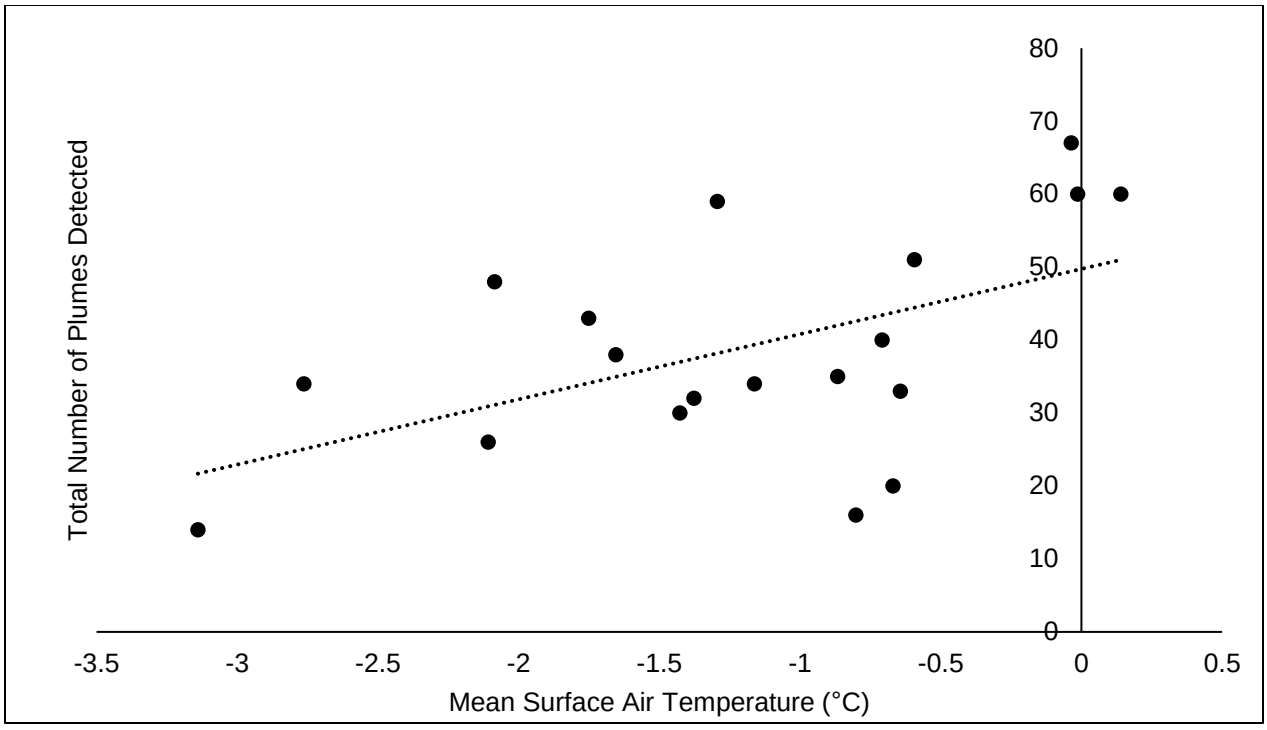

Figure 5.9: Mean surface air temperatures from June to September for 1997-2015 produced from NCEP/NCAR Reanalysis data (1981-2010 climatology) compared to the total number of annual plumes detected for all glaciers in the study. Source: Kalnay et al., 1996.

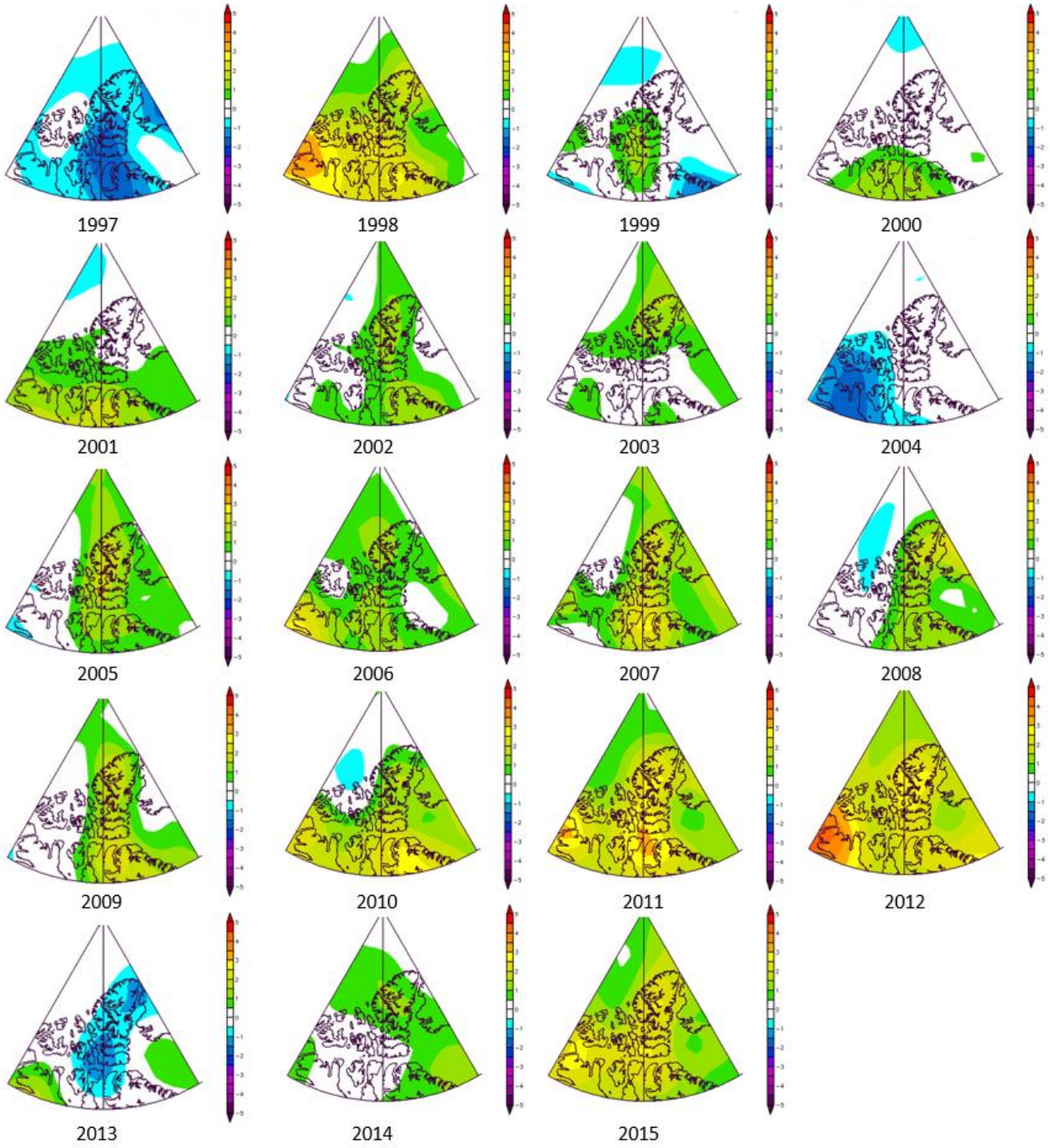

Figure 5.10: NCEP/NCAR Reanalysis data showing 1981-2010 climatology surface temperature anomalies for June to September from 1997 to 2015 over the Queen Elizabeth Islands. Source: Kalnay et al., 1996.

Chapter 6: Conclusion

This study presents the first comprehensive assessment of iceberg production from glaciers around the Prince of Wales Icefield, including the identification of timing and magnitude of individual plume events in relation to local sea ice, tidal, oceanographic and atmospheric conditions. The study used a total of 8426 SAR and optical satellite images from 1997 to 2015 to identify iceberg plume events for 40 tidewater glaciers with a terminus width of >1 km, of which 25 glaciers were found to be active iceberg producers.

Two of 40 glaciers (Trinity and Wykeham) in the POW were found to be particularly active in terms of iceberg production. On a regional basis, there is a strong connection between the velocity of glaciers and the number of iceberg calving events that they produce, with Trinity and Wykeham Glaciers currently the fastest flowing glaciers in the Canadian Arctic. The temporal variability in iceberg production from these glaciers coincides with interannual variations in their velocity as identified by Van Wychen et al. (2016). A gradual increase in velocity for both glaciers from about 1999 to 2007 followed by a more rapid acceleration from 2009 to 2015 coincides with a slight decrease in plume events over time between 1998 and 2008, following by a more productive period since 2009 with a general increase toward the present day. This idea is further supported by the significant terminus retreat observed from 1959-2015 in this study. It is likely that the increased movement of thinner and less stable crevassed ice towards the terminus of the glacier as a result of higher velocities contributes to the amount of ice being discharged from Trinity and Wykeham glaciers as well as other more active glaciers in the study. No clear relationship was found between years of high terminus retreat and a high number of detected plume events. For example, between 2011 and 2012, Trinity Glacier retreated ~1 km, however there was no significant increase in the number of iceberg plumes detected that year. The production of plume events is therefore likely

more closely linked to ice moving past the terminus instead of terminus retreat. The remaining glaciers in the study which did not undergo significant increases in speed over the time period also did not produce the high numbers of iceberg plumes as were seen from Trinity and Wykeham glaciers.

A significant finding from this study is that the presence of landfast sea ice at the terminus of tidewater glaciers is a primary controlling factor on the annual timing of iceberg calving from all glaciers. The production of icebergs increases when open water is present and decreases when landfast sea ice and an ice mélange form at the terminus. These results are consistent with the findings of others (Reeh et al., 2001; Pope et al., 2012; Carr et al., 2013) and most relevant to the findings of Herdes et al. (2012) who conducted a similar study on two glaciers on Devon Ice Cap and upon which the methodology of this work was based. Findings also showed that while calving events during the winter when sea ice is present are less common, they do still occur. There was no clear relationship identified between daily tidal cycles or ocean temperatures and the production of icebergs from POW glaciers. Since data used in this analysis was derived from models and through reanalysis, results of this study would benefit from the use of observational tidal and climate data to determine with high accuracy whether a relationship exists between the production of icebergs and ocean temperature, air temperature and daily tidal cycles.

These findings hold importance for the impacts of climate change in the region. Past studies have shown that sea ice extent and thickness are declining in all regions of the Canadian Arctic and the open water season is lengthening. This suggests that in the future there will be less sea ice present at the terminus of CAA glaciers to act as a barrier between the open ocean and the calving front, which could potentially lead to an increase in icebergs being discharged into Canadian waters. Increased presence of icebergs in Canadian waters can pose a threat for shipping lanes and offshore

oil exploration projects in addition to contributing to sea level rise if they result in more ice being discharged from the land.

Future work would benefit from a comparison between ScanSAR wide mode satellite imagery data and regular (e.g., hourly) time-lapse photos of glacier termini to determine the accuracy of using remote sensing to detect iceberg plumes. Plume analysis could also be developed into automatic detection to reduce the subjectivity of manual analysis. However, manual analysis of satellite scenes allowed for more accurate identification of features such as differentiating between ice mélange and freshly calved iceberg plumes in the winter. Time-lapse cameras and dGPS stations installed at Trinity Glacier in 2016 by the Laboratory for Cryospheric Research continue to collect data on the timing of plume events, terminus retreat and glacier velocity that could be used to further analyze the results of this study. This data will create a longer, more accurate record that can be used to further our understanding of the processes that drive iceberg production from this region and how these are continuing to change over time.

Chapter 7: References

Amundson, J. M., Fahnestock, M., Truffer, M., Brown, J., Lüthi, M. P. and Motyka, R. J. (2010) Ice mélange dynamics and implications for terminus stability, Jakobshavn Isbræ, Greenland. *Journal of Geophysical Research*, 115(F1), 1-12.

Andersen, M.L., Larsen, T.B., Nettles, M., Elosegui, P., van As, D., Hamilton, G.S., Stearns, L.A., Davis, J.L., Ahlstrøm, A.P., de Juan, J., Ekström, G., Stenseng, L., Khan, S.A., Forsberg, R. and Dahl-Jensen, D. (2010) Spatial and temporal melt variability at Helheim Glacier, East Greenland, and its effect on ice dynamics. *Journal of Geophysical Research*, 115(F04041), doi: 10.1029/2010JF001760.

Benn, D. I., Hulton, N. R. J., and Mottram, R. H., (2007a) 'Calving laws', 'sliding laws' and the stability of tidewater glaciers. *Annals of Glaciology*, 46, 123-130.

Benn, D.I., Warren, C.R. and Mottram, R.H. (2007b) Calving processes and the dynamics of calving glaciers. *Earth-Science Reviews,* 82, 143-179.

Canadian Ice Service (CIS) (2005) MANICE. Online. Available at https://www.canada.ca/en/environment-climate-change/services/weather-manuals-documentation/manice-manual-of-ice.html

Carr, R.J., Vieli, A. and Stokes, C. (2013) Influence of sea ice decline, atmospheric warming, and glacier width on marine-terminating outlet glacier behavior in northwest Greenland at seasonal to interannual timescales. *Journal of Geophysical Research: Earth Surface*, 118, 1-17, doi: 10.1002/jgrf.20088.

Cohen, J., Screen, J. A., Furtado, J. C., Barlow, M., Whittleston, D., Coumou, D., Francis, J., Dethloff, K., Entekhabi, D., Overland, J. and Jones, J. (2014) Recent Arctic amplification and extreme mid-latitude weather. *Nature Geoscience,* 7, 627-637.

Galley, R.J., Else, B.G.T., Lukovich, J. V., Howell, S.E.L. and Barber, D.G. (2012) Landfast Sea Ice Conditions in the Canadian Arctic: 1983-2009. *Arctic*, 65(2), 133-144.

Harig, C., and Simons, F. J. (2016) Ice mass loss in Greenland, the Gulf of Alaska, and the Canadian Archipelago: Seasonal cycles and decadal trends. *Geophysical Research Letters*, 43 (7), 3150-3159. http://doi.org/10.1002/2016GL067759

Herdes, E., Copland, L., Danielson, B. and Sharp, M. (2012) Relationships between iceberg plumes and sea-ice conditions on northeast Devon Ice Cap, Nunavut, Canada. *Annals of Glaciology*, 53(60), 1-9, doi: 10.3189/2012AoG60A163.

Higgins, A. K. (1991) North Greenland glacier velocities and calf ice production. *Polarforschung*, 60(1), 1-23.

Howat, I.M., Box, J.E., Ahn, Y., Herrington, A. and McFadden, E.M. (2010) Seasonal variability in the dynamics of marine-terminating outlet glaciers in Greenland. *Journal of Glaciology*, 56(198), 601-613.

Howell, S.E.L., Wohlleben, T., Dabboor, M., Derksen, C., Komarov, A., Pizzolato, L. (2013) Recent changes in the exchange of sea ice between the Arctic Ocean and the Canadian Arctic Archipelago. J. Geophys. Res. Oceans., 118, doi: 10.1002/jgrc.20265.

Joughin, I., Howat, I.M., Fahnestock, M., Smith, B., Krabill, W., Alley, R.B., Stern, H. and Truffer, M. (2008) Continued evolution of Jakobshavn Isbrae following its rapid speedup. *Journal of Geophysical Research*, 113(F04006), doi: 10.1029/2008JF001023.

Kalnay, E., Kanamitsu, M., Kistler, R., Collins, W., Deaven, D., Gandin, L., Iredell, M., Saha, S., White, G., Woollen, J., Zhu, Y., Chelliah, M., Ebisuzaki, W., Higgins, W., Janowiak, J., Mo, K.C., Ropelewski, C., Wang, J., Leetmaa, A., Reynolds, R., Jenne, R. and Joseph D. (1996) The NCEP/NCAR 40-Year Reanalysis Project. *Bulletin of the* American *Meteorological* Society, 77, 437–471.

Kwok, R. and Rothrock, D. A. (2009) Decline in Arctic sea ice thickness from submarine and ICESat records: 1958–2008. *Geophysical Research Letters*, 36(15), 1-5.

Lindsay, R and Schweiger, A. (2015) Arctic sea ice thickness loss determined using subsurface, airfcraft and satellite observations. *The Cryosphere*, 9, 269-283, doi:10.5194/tc-9-269-2015.

Mahoney, A. R., Eicken, H., A. Gaylord, G. and Shapiro, L. (2007) Alaska landfast sea ice: Links with bathymetry and atmospheric circulation. *Journal of Geophysical Research-Oceans*, 112 (C02001), doi: 10.1029/2006JC003559.

Maslanik, J., Stroeve, J., Fowler, C. and Emery, W. (2011) Distribution and trends in Arctic sea ice age through spring 2011. *Geophysical Research Letters.* 38(13), doi: 10.1029/2011GL047735.

Millan, R., Mouginot, J., Rignot, E. (2017) "Mass budget of the glaciers and ice caps of the Queen Elizabeth Islands, Canada, from 1991 to 2015." *Environmental Research Letters*, 12(2), (doi: 10.1088/1748-9326aa5b04)

Moon, T. and Joughin, I. (2008) Changes in ice front position on Greenland's outlet glaciers from 1992 to 2007. *Journal of Geophysical Research*, 113(F2), F02022. (doi: 10.1029/2007JF000927.)

Moon, T., Joughin, I. and Smith, B. (2015) Seasonal to multiyear variability of glacier surface velocity, terminus position, and sea ice/ice mélange in northwest Greenland. *J. Geophys. Res. Earth Surf.*, 120, 818–833. doi: 10.1002/2015JF003494.

Motyka, R. J., Hunter, L., Echelmeyer, K. and Connor, C. (2003) Submarine melting at the terminus of a temperate tidewater glacier, LeConte Glacier, Alaska, U.S.A. *Annals of Glaciology*, 36, 57–65.

Motyka, R. J., Truffer, M., Fahnestock, M. , Mortensen, J., Rysgaar, S. and Howat, I.M. (2011) Submarine melting of the 1985 Jakobshavn Isbræ floating tongue and the triggering of the current retreat. *Journal of Geophysical Research*, 116 (F01007), doi: 10.1029/2009JF001632.

O'Leary, M. and Christoffersen, P. (2013) Calving of tidewater glaciers amplified by submarine frontal melting. *The Cryosphere*, 7, 119-128.

Park, D-S.R., Lee S., and Feldstein, S.B. (2015) Attribution of the Recent Winter Sea Ice Decline over the Atlantic Sector of the Arctic Ocean. *Journal of Climate*, 28, 4027–4033. doi: http://dx.doi.org/10.1175/JCLI-D-15-0042.1

Pimentel, S., Flowers, G.E., Sharp, M.J., Danielson, B., Copland, L., Van Wychen, W., Duncan, A. and Kavanaugh, J. (2017) Modelling intra-annual dynamics of a major marine-terminating Arctic glacier**.** *Annals of Glaciology*, doi: 10.1017/aog.2017.23.

Polyakov, I., Walsh, J. and Kwok, R. (2012) Recent changes of arctic multiyear sea ice coverage and the likely causes. *Bulletin of the American Meteorological Society*, 93, 145–151, doi: 10.1175/BAMS-D-11-00070.1.

Pope, S., Copland, L. and Mueller, D. (2012) Loss of multiyear landfast sea ice from Yelverton Bay, Ellesmere Island, Nunavut, Canada. *Arctic, Antarctic, and Alpine Research*, 44(2), 210-221.

Reeh, N., Højmark, H., Higgins, A.K. and Weidick, A. (2001) Sea ice and the stability of north and northeast Greenland floating glaciers. *Annals of Glaciology*, 33, 474-480.

Sakov, P., Counillon, F. Bertino, L., Lisæter, K.A., Oke, P.R. and Korablev, A. (2012) TOPAZ4: An ocean-sea ice data assimilation system for the North Atlantic and Arctic, *Ocean Science*., 8(4), 633–656, doi:10.5194/os-8-633-2012.

Screen, J. and Simmonds, I. (2010) The central role of diminishing sea ice in the recent Arctic temperature amplification. *Nature*, 464, 1334–1337

Serreze, M.C. and Barry, R.G. (2011) Processes and Impacts of Arctic Amplification: A Research Synthesis. *Global and Planetary Change*, 77, 85-96. doi: 10.1016/j.gloplacha.2011.03.004

Serreze, M.C. and Stroeve, J. (2015) Arctic sea ice trends, variability and implications for seasonal ice forecasting. *Phil. Trans. R. Soc*. A 373: 20140159. http://dx.doi.org/10.1098/rsta.2014.0159
Screen, J. and Simmonds, I. (2010) The central role of diminishing sea ice in the recent Arctic temperature amplification. *Nature* 464, 1334–1337

Sharp, M., Burgess, D.O., Cawkwell, F., Copland, L., Davis, J.A., Dowdeswell, E.K., Dowdeswell, J.A., Gardner, A.S., Mair, D., Wang, L., Williamson, S.N., Wolken, G. J. and Wyatt, F. (2014) Remote sensing of recent glacier changes in the Canadian Arctic. In: Kargel, J.S., Leonard, G.J., Bishop, M.P., Kääb, A. and Raup, B.H. (eds). *Global Land Ice Measurements from Space*, Ch. 9, pp. 205-228. Praxis-Springer. doi: 10.1007/978-3-540-79818-7_9.

Simmonds, I. (2015) Comparing and contrasting the behaviour of Arctic and Antarctic sea ice over the 35 year period 1979–2013. *Annals of Glaciology*, *56*(69), 18–28. doi:10.3189/2015AoG69A909.

Stroeve, J. C., Markus, T., Boisvert, L., Miller, J., and Barrett, A. (2014) Changes in Arctic melt season and implications for sea ice loss. *Geophysical Research Letters*, 41, 1216–1225, doi:10.1002/2013GL058951.

Stroeve, J., Serreze, M., Drobot, S., Gearheard, S., Holland, M., Maslanik, J., Meier, W., and Scambos, T. (2008) Arctic Sea Ice Extent Plummets in 2007. *Eos Trans. AGU*, 89(2), 13–14, doi:10.1029/2008EO020001.

Van Wychen, W., Copland, L., Gray, L., Burgess, D., Danielson, B. and Sharp, M. (2012) Spatial and temporal variation of ice motion and ice flux from Devon Ice Cap, Nunavut, Canada. *Journal of Glaciology*, 58(210), 657-664.

Van Wychen, W., Burgess, D.O., Gray, L., Copland, L., Sharp, M., Dowdeswell, J. and Benham, T. (2014) Glacier velocities and dynamic ice discharge from the Queen Elizabeth Islands, Nunavut, Canada**.** *Geophysical Research Letters*, 41(2), 484-490. doi: 10.1002/2013GL058558

Van Wychen, W., Davis, J., Burgess, D.O., Copland, L., Gray, L., Sharp, M. and Mortimer, C. (2016) Characterizing interannual variability of glacier dynamics and dynamic discharge (1999-2015) for the ice masses of Ellesmere and Axel Heiberg Islands, Nunavut, Canada. *Journal of Geophysical Research – Earth Surface*, 121, doi: 10.1002/2015JF003708

Vieli, A. and Nick, F.M. (2011) Understanding and modelling rapid dynamic changes of tidewater outlet glaciers: issues and implications. *Surveys in Geophysics*, 32(4-5), 437-458.

Walter, J. I., Box, J. E., Tulaczyk, S., Brosky, E. E., Howat, I. M., Ahn, Y., and Brown, A., (2012) Oceanic mechanical forcing of a marine-terminating Greenland glacier. *Annals of Glaciology*, 53(60), 181-192.

Wang, M. and Overland, J. E. (2009) A sea ice free summer Arctic within 30 years? *Geophysical Research Letters*, 36(7), 1-5.

White, A., Copland, L., Mueller, D. and Van Wychen, W. (2015) Assessment of historical changes (1959-2012) and the causes of recent break-ups of the Petersen ice shelf, Nunavut, Canada. *Annals of Glaciology, 56(69)*, 65-76. doi: 10.3189/2015AoG69A687

Williamson, S., Sharp, M., Dowdeswell, J. and Benham, T. (2008) Iceberg calving rates from northern Ellesmere Island ice caps, Canadian Arctic, 1999-2003. *Journal of Glaciology*, 54(186), 391-400.